ChemPubSoc Europe

DOI: 10.1002/ejic.201600722

EurJIC European Journal of Inorganic Chemistry

Full Paper

Mixed Donor Ligands

Homo- and Heterodinuclear Rh and Ir Complexes Supported by SN_n Mixed-Donor Ligands (n = 2–4). Stereochemistry and Coordination-Site-Exchange Reactions of Cp*M (M = Rh, Ir) Units

Takayuki Nakajima,*[a] Yuki Kawasaki,[a] Bunsho Kure,[a] and Tomoaki Tanase*[a]

Abstract: A series of SN_n mixed-donor ligands [n = 2: $H_2NC_2H_4SCH_2$-2-pyridyl (2-NSpy) (**1a**), $H_2NC_2H_4SCH_2$-4-pyridyl (4-NSpy) (**1b**), n = 3: 2-pyridylCH$_2$NHC$_2$H$_4$SCH$_2$-2-pyridyl (2-pyNSpy) (**2**), n = 4: (2-pyridylCH$_2$)$_2$NC$_2$H$_4$SCH$_2$-2-pyridyl (2-py$_2$NSpy) (**3**)] was utilized to support homo- and heterodinuclear complexes including Cp*M^{III} units (M = Rh, Ir; Cp* = pentamethylcyclopentadienyl). Reactions of [Cp*MCl$_2$]$_2$ with 2-pyNSpy (**2**), 2-py$_2$NSpy (**3**), and 4-NSpy (**1b**) afforded homodinulear complexes, [(Cp*MCl)(2-pyNSpy)(Cp*MCl)](PF$_6$)$_2$ [M = Rh (**5a**), Ir (**5b**)], [(Cp*M)(2-py$_2$NSpy)(Cp*MCl)](PF$_6$)$_3$ [M = Rh (**6a**), Ir (**6b**)], [(Cp*MCl)(4-NSpy)(Cp*MCl$_2$)]Cl [M = Rh (**8a**), Ir (**8b**)]. Heterodinuclear complexes [(Cp*MCl)(4-NSpy)(Cp*M′Cl$_2$)]Cl [M, M′ = Rh, Ir (**8c**), Ir, Rh (**8d**)] were prepared using mononuclear complexes [(Cp*MCl)(4-NSpy)]Cl [M = Rh (**7a**), Ir (**7b**)] reacted with [Cp*MCl$_2$]$_2$ (M = Ir, Rh), respectively. Complexes **5**–**8** were characterized by X-ray crystallography to determine the configurations around the M, M′, S, and N centers. The solid-state structures of **6** are retained in acetonitrile solution whereas four diastereomers are generated in the case of **5** due to low stereoselectivity around the coordinated amine nitrogen atom, in contrast to the sulfur atom. Heterodinuclear complexes **8c**,**d** are unstable in solution at 55 °C, readily affording mixtures of **8a**–**d** via intra- and intermolecular coordination-site-exchange reactions of Cp*M fragments between the SN moiety and the py site. In order to evaluate the selectivity of Cp*M fragments for the SN and py coordination sites, several competitive reactions of [Cp*MCl$_2$]$_2$ (M = Rh, Ir) with $H_2NC_2H_4SCH_2C_6H_5$ (NSph) (**4**) and/or 4-methylpyridine (4-Mepy) were carried out to demonstrate predominant formation of iridium complexes **9b** and **10b** among [(Cp*MCl)(NSph)]Cl [M = Rh (**9a**), Ir (**9b**)] and [(Cp*MCl)(4-Mepy)]Cl [M = Rh (**10a**), Ir (**10b**)]. These reactions indicated higher affinity of the Cp*Ir fragment to both the NS and py sites relative to the rhodium analogue.

Introduction

Design efforts focused on multidentate ligands have provided fundamental progress in creating new functional complexes and materials related to a variety of useful applications in organometallic and inorganic chemistry.[1] In particular, mixed-donor multidentate ligands are of considerable interest since they show additional abilities such as hemilabile chelating and bridging effects that are not accomplished by simple and classical monodentate ligands.[2,3] With an aim of utilizing hard and soft donor combinations, a number of studies have been carried out on metal complexes supported by nitrogen and sulfur mixed-donor ligands in the fields of bioinorganic and organometallic chemistry.[4] However, half-metallocene complexes with SN chelating ligands including Cp*M fragments (M = Rh, Ir, Ru etc., Cp* = pentamethylcyclopentadienyl) are limited only to just a few examples.[5,6] However, such three-legged pianostool complexes are widely utilized as catalyst precursors in organic transformations and their four-coordinate, pseudo-octahedral geometry has facilitated studies on stereochemistry with respect to the metal center.[7]

Recently, we intended to construct functional dinuclear metal centers supported by hemilabile multidentate ligands, and prepared dinuclear Cp*M^{III} (M = Rh, Ir) complexes connected by a series of tetradendate P_2N_2 ligands, {(Cp*MCl)$_2$[*meso*- or *rac*-2-pyCH$_2$P(Ph)(CH$_2$)$_n$P(Ph)CH$_2$-2-py]}-(PF$_6$)$_2$ (M = Rh, Ir), where the stereo-structures around two metal centers are influenced by configurations of the coordinated P atoms and the length of the central methylene chain.[8] In the present study, new SN_n mixed-donor ligands [n = 2: $H_2NC_2H_4SCH_2$-4-pyridyl (4-NSpy) (**1b**), n = 3: 2-pyridylCH$_2$NHC$_2$H$_4$SCH$_2$-2-pyridyl (2-pyNSpy) (**2**), n = 4: (2-pyridylCH$_2$)$_2$NC$_2$H$_4$SCH$_2$-2-pyridyl (2-py$_2$NSpy) (**3**)] were synthesized based on a cysteamine unit, and were treated with [Cp*MCl$_2$]$_2$ (M = Rh, Ir) to afford homo- and heterodinuclear Cp*M^{III} complexes supported by the SN_n ligands, [(Cp*MCl)-(2-pyNSpy)(Cp*MCl)](PF$_6$)$_2$ [M = Rh (**5a**), Ir (**5b**)], [(Cp*M)-(2-py$_2$NSpy)(Cp*MCl)](PF$_6$)$_3$ [M = Rh (**6a**), Ir (**6b**)], and [(Cp*MCl)(4-NSpy)(Cp*M′Cl$_2$)]Cl [M, M′ = Rh, Rh (**8a**), Ir, Ir (**8b**),

[a] *Department of Chemistry, Faculty of Science, Nara Women's University, Kitauoya-nishi-machi, Nara 630-8506, Japan*
E-mail: t.nakajima@cc.nara-wu.ac.jp
tanase@cc.nara-wu.ac.jp
http://www.chem.nara-wu.ac.jp/~tanase/TanaseGroup/

Supporting information for this article is available on the WWW under http://dx.doi.org/10.1002/ejic.201600722.

Rh, Ir (**8c**), Ir, Rh (**8d**)]; these were characterized by spectroscopic and crystallographic analyses to elucidate configurational selectivity around the M, M′, S, and N centers and the coordination-site-exchange reactions of the Cp*M units.

Results and Discussion

Synthesis of SN_n Mixed-Donor Ligands 1–4

The SN_n mixed-donor ligands **1**–**4** were synthesized as shown in Scheme 1. Tridentate SN_2 ligands **1a**,**b** (2-, and 4-NSpy) were prepared by the reaction of cysteamine hydrochloride with 2- or 4-(chloromethyl)pyridine in the presence of $NaHCO_3$ according to previously published procedures.[9] Reductive amination of **1a** and 2-pyridinealdehyde in the presence of $NaBH_4$ afforded tetradentate SN_3 ligand **2** (2-pyNSpy) in 91 % yield, which was further reacted with 2-(chloromethyl)pyridine to give SN_4 ligand **3** (2-py_2NSpy) in 73 % yield. SN ligand **4** (NSPh) was prepared by the reaction of cysteamine hydrochloride with benzyl chloride in 76 % yield.

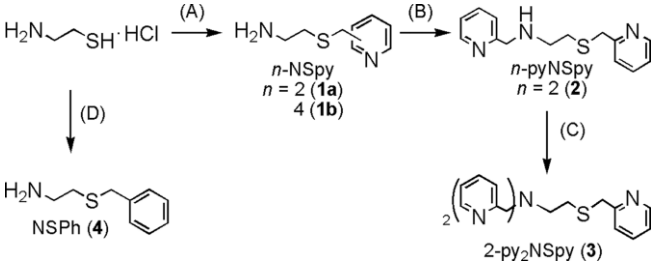

Scheme 1. Preparations of mixed-donor SN ligands **1**–**4**. (A) *x*-(chloromethyl)pyridine, $NaHCO_3$ in EtOH; (B) **1a**, pyridine-2-carbaldehyde, $NaBH_4$ in MeOH; (C) 2-(chloromethyl)pyridine, $NaHCO_3$ in EtOH; (D) benzyl chloride, $NaHCO_3$ in EtOH.

Homodinuclear Rhodium and Iridium Complexes Supported by SN_3 and SN_4 Ligands (2-pyNSpy and 2-py_2NSpy)

Reactions of $[Cp^*MCl_2]_2$ (M = Rh, Ir) with 1 equiv. of 2-py_2NSpy (**3**) in the presence of NH_4PF_6 in MeOH at room temperature gave homodinuclear $[(Cp^*MCl)(2\text{-}py_2NSpy)(Cp^*MCl)](PF_6)_3$ [M = Rh (**6a**), Ir (**6b**)] in 36 and 61 % yields, respectively (Scheme 2). The structures of **6a**,**b** were determined by X-ray crystallography to be isomorphous with each other; ORTEP views for the complex cations of **6a**,**b** are given in Figure 1 and Figure S1 (Supporting Information), respectively. The complex cations of **6** are comprised of {Cp*MCl} and {Cp*M} units chelated by 2-$pyCH_2S$ and 2-py_2CH_2N moieties in the two ends of ligand **3**, respectively, to form three-legged piano-stool structures. The metal–to–ligand distances are almost identical irrespective of the metal species Rh or Ir; M–C = 2.148(3)–2.205(4) Å (av. 2.175 Å) (**6a**), 2.158(5)–2.217(6) Å (av. 2.190 Å) (**6b**); M–N = 2.103(3)–2.198(2) Å (av. 2.131 Å) (**6a**), 2.100(5)–2.193(4) Å (av. 2.131 Å) (**6b**); M–Cl = 2.4021(13) (**6a**), 2.395(2) Å (**6b**); M–S = 2.3402(8) (**6a**), 2.3236(12) Å (**6b**). Since the M1 and S1 centers in **6** are stereogenic, two diastereomers R_MR_S/S_MS_S and R_MS_S/S_MR_S are potentially generated. In fact, X-ray analysis of **6** clearly indicates that the absolute configurations around M1 and S1 centers are R_MR_S/S_MS_S with the $C_2H_4N(CH_2py)_2$ substituent of S1 atom and Cl1 ligand attached to the Rh1 center located in a *syn* arrangement with respect to the Rh1–S1 bond [dihedral angle Cl1–Rh1–S1–$C_{ethylene}$ = 2.13(4)° (**6a**), 0.90(8)° (**6b**)]. A similar stereo-arrangement is also observed in $[(Cp^*MCl)L](PF_6)$ [M = Rh, Ir; L = 2-(pyridine-2-ylmethylthio)benzoic acid, 2-(pyridine-2-ylthiomethyl)pyridine, 8-methylthioquinoline] supported by SN chelate ligands.[6a,d,e] In our previous studies on dinuclear Cp*Rh and Cp*Ir complexes supported by a series of NPPN ligands, 2-$pyCH_2(Ph)P(CH_2)_nP(Ph)CH_2$-2-py (*n* = 2–4), all characterized complexes $\{(Cp^*MCl)_2[2\text{-}pyCH_2(Ph)P(CH_2)_nP(Ph)CH_2\text{-}2\text{-}py]\}(BF_4)_2$ exhibited a similar stereoselectivity as observed in **6**, where the methylene unit on the phosphorus atom and chloride ligand are in a *syn*-arrangement with respect to M–P bond.[8] The ^1H and ^{13}C NMR spectra of **6** show the presence of only two signals for the Cp* rings [^1H NMR: δ = 1.72 (15 H), 1.64 (15 H) ppm (**6a**), δ = 1.72 (15 H), 1.59 (15 H) ppm (**6b**). ^{13}C NMR: δ = 101.4 (d, J_{CRh} = 7 Hz), 100.6 (d, J_{CRh} = 8 Hz), 10.1, 9.9 ppm (**6a**), δ = 93.7, 92.0, 9.0, 8.9 ppm (**6b**)] and the ESI–MS spectra in CH_3CN exhibited the parent peaks for $\{[Cp^*_2Rh_2Cl(2\text{-}pyNSpy_2)](PF_6)_2\}^+$ (*m/z* 1151.34) and $\{[Cp^*_2Ir_2Cl(2\text{-}pyNSpy_2)](PF_6)_2\}^+$ (*m/z* 1331.21), indicating that the solid-state structures

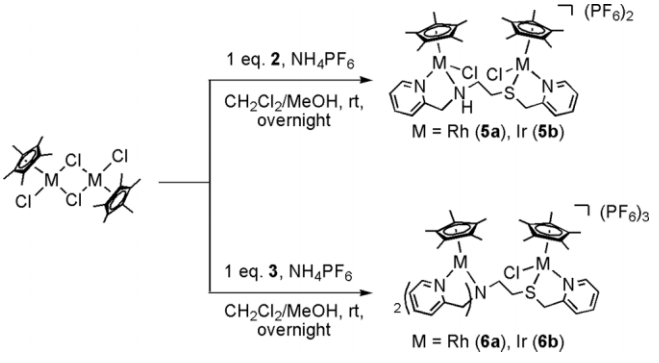

Scheme 2. Preparations of $[(Cp^*MCl)(2\text{-}pyNSpy)(Cp^*MCl)](PF_6)_2$ (**5**) and $[(Cp^*M)(2\text{-}py_2NSpy)(Cp^*MCl)](PF_6)_3$ (**6**) [M = Rh (**a**), Ir (**b**)].

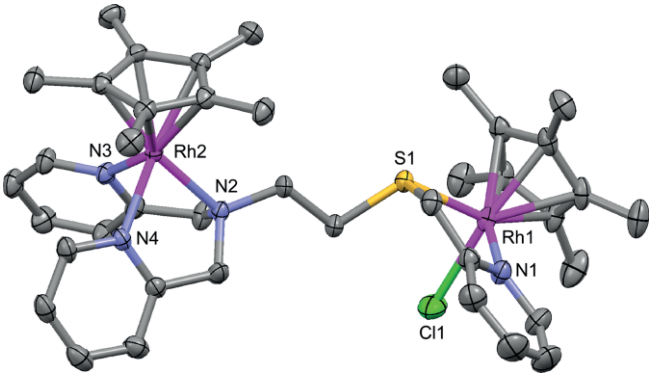

Figure 1. ORTEP diagram for the complex cation of **6a** with the atomic numbering scheme. The thermal ellipsoids are drawn at the 40 % probability level, and the C–H hydrogen atoms are omitted for clarity.

are retained in solution. It should be noted that, in the mononuclear complexes supported by thioether and pyridyl donor multidentate ligands, sulfur inversion was often observed and several invertomers exist in solution.[10] Contrary to the present case, inversion of the sulfur atom was not observed in **6**, which might be rationalized on the basis of the bulky substituents at both metal and sulfur centers.

The treatment of $[Cp^*MCl_2]_2$ (M = Rh, Ir) with 1 equiv. of 2-pyNSpy (**2**) in the presence of NH_4PF_6 in MeOH afforded homodinuclear $[(Cp^*MCl)(2\text{-pyNSpy})(Cp^*MCl)](PF_6)_2$ [M = Rh (**5a**), Ir (**5b**)] in 76 and 86 % yields, respectively (Scheme 2). The crystal structure of **5a** was refined with a disorder model in which the central SCH_2CH_2N fragment locates at two sites, each relating with C_i symmetry with 0.5 occupancy (one set of the disordered structures is illustrated for clarity) and reveals that two Cp*RhCl fragments were chelated by 2-pyCH_2S and 2-pyCH_2N moieties in the two ends of ligand **2** without any metal–metal interactions [Rh1···Rh1* 6.2224(8) Å] (Figure 2). The absolute configurations around the Rh1, S1, N2*, and Rh1* atoms are $R_{Rh1}R_{S1}R_{N2*}R_{Rh1*}/S_{Rh1}S_{S1}S_{N2*}S_{Rh1*}$ out of eight possible diastereomers. The configurations around the Rh1 and S1 centers are the same as in **6**, and those around the N2*and Rh1* atoms are also regulated similarly with *syn*-periplanar geometries for Cl2* ligand and the C_2H_4SR unit [Cl1–Rh1–S1–$C_{ethylene}$ 0.5(2)°, Cl2–Rh1*–N2*–$C_{ethylene}$ 4.3(12)°]; the opposite stereo-configuration was observed in the case of $[Cp^*IrCl(pyam)](SbF_6)$ (pyam = *R*-2-pyCH_2NHCHPhMe) supported by a chiral pyridylamino ligand.[11] The ^{1}H NMR spectrum of **5a** (Figure S10, Supporting Information) indicates that four diastereomers exist in solution as reflected by the presence of four sets of two singlets each for Cp* rings with a ratio of 46:28:20:6 which remains unchanged at room temperature for several days. On the other hand, the ^{1}H NMR spectrum of **5b** (Figure S11, Supporting Information) shows, at first, two sets of two singlet peaks each for Cp* rings in a ratio of 83:17. After keeping this sample at room temperature for several days, two new sets of peaks appeared and increased gradually as two of the original signals decreased leading to formation of four isomers in a ratio of 30:29:25:16. As for the configurations of four isomers, the configurations around the M1 and S1 centers in **5** were postulated to be constrained to $R_{M1}R_{S1}/S_{M1}S_{S1}$ by analogy with **6** and $[(Cp^*MCl)L](PF_6)$ [M = Rh, Ir; L = 2-(pyridine-2-ylmethylsulfanyl)benzoic acid].[6a] In contrast, those for the M1* and N2* centers are presumably not constrained to afford both $R_{N2*}R_{M1*}/S_{N2*}S_{M1*}$ and $R_{N2*}S_{M1*}/S_{N2*}R_{M1*}$ diastereomers, in the light of the fact that four diastereomers were observed for related complex $[Cp^*IrCl(pyam)](SbF_6)$ in solution.[11] After all, four diastereomers, $R_{M1}R_{S1}R_{N2*}R_{M1*}/S_{M1}S_{S1}S_{N2*}S_{M1*}$, $R_{M1}R_{S1}S_{N2*}S_{M1*}/S_{M1}S_{S1}R_{N2*}R_{M1*}$, $R_{M1}R_{S1}R_{N2*}S_{M1*}/S_{M1}S_{S1}S_{N2*}R_{M1*}$, and $R_{M1}R_{S1}S_{N2*}R_{M1*}/S_{M1}S_{S1}R_{N2*}S_{M1*}$, can be generated in solution for **6a**,**b**.

Mononuclear Rhodium and Iridium Complexes Supported by SN_2 Ligand (4-NSpy)

When $[Cp^*MCl_2]_2$ (M = Rh, Ir) was treated with 3 equiv. of 4-NSpy (**1b**) in CH_2Cl_2 at room temperature, mononuclear complexes $[(Cp^*MCl)(4\text{-NSpy})]Cl$ [M = Rh (**7a**), Ir (**7b**)] were obtained in 78 and 81 % yields, respectively (Scheme 3). The crystal structures of **7a**,**b** are isomorphous with each other, having a three-legged piano-stool structure around M center coordinated by 4-NSpy ligand via amine nitrogen and sulfur atoms to form a five-membered chelate ring, the pyridyl nitrogen being uncoordinated [M1–Cl1 2.3958(8) Å (**7a**), 2.397(2) Å (**7b**); M1–S1 2.3824(9) Å (**7a**), 2.358(2) Å (**7b**); M1–N1 2.126(2) Å (**7a**), 2.132(4) Å (**7b**)] (Figure 3 for **7a** and Figure S2 in Supporting Information for **7b**). The configurations around the M1 and S1 centers are the same as those in **5** and **6**, where chloride ligand Cl1 and pyridylmethyl substituent on S1 are located in *syn*-periplanar geometry with respect to M1–S1 bond [Cl1–M1–S1–C_{CH2py} −3.95(3)° (**7a**), −5.78(7)° (**7b**)]. Only one diastreomer of **7** exists in CD_3OD solution at room temperature, which was

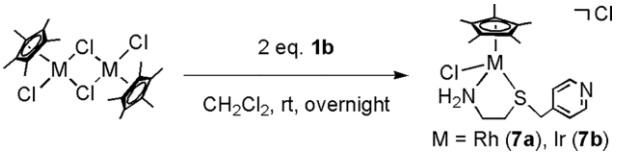

Scheme 3. Preparations of [(Cp*MCl)(4-NSpy)]Cl (**7**) [M = Rh (**a**), Ir (**b**)].

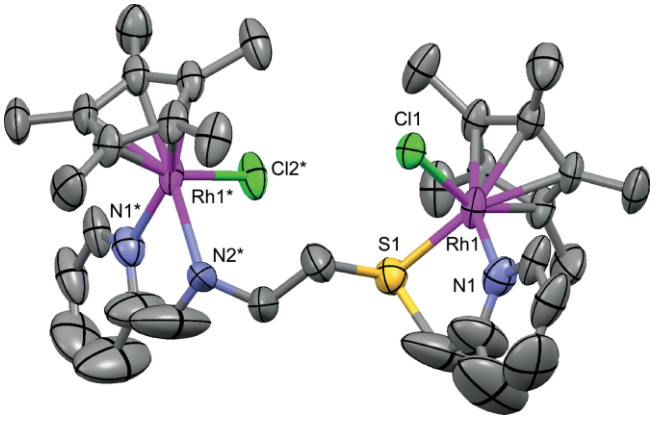

Figure 2. ORTEP diagram for the complex cation of **5a** with the atomic numbering scheme. The thermal ellipsoids are drawn at the 40 % probability level, and the hydrogen atoms are omitted for clarity.

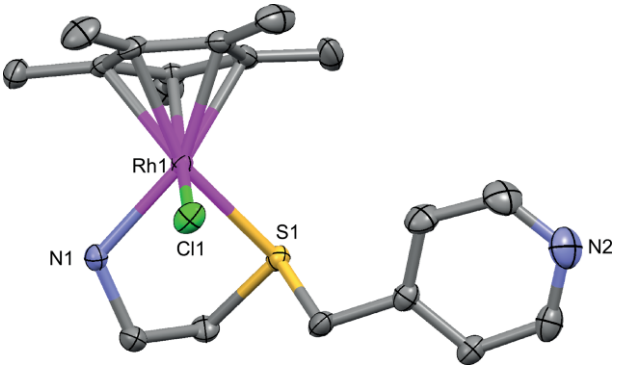

Figure 3. ORTEP diagram for the complex cation of **7a** with the atomic numbering scheme. The thermal ellipsoids are drawn at the 40 % probability level, and the hydrogen atoms are omitted for clarity.

confirmed by the presence of only one singlet peaks for Cp* protons [δ = 1.62 (**7a**), 1.62 (**7b**) ppm] in the ^{1}H NMR spectra. The ESI-MS spectra in CH_3CN exhibited the parent peaks for $[Cp^*MCl(NSpy)]^+$ at *m/z* 441.07 (M = Rh) and 531.20 (M = Ir). These indicate that the solid-state structures were retained in solution.

Homo- and Heterodinuclear Rhodium and Iridium Complexes Supported by SN_2 Ligand (4-NSpy)

Treatments of [(Cp*MCl)(4-NSpy)]Cl (**7**) with 0.5 equiv. of respective dimer, $[Cp^*MCl_2]_2$ (M = Rh for **8a**, Ir for **8b**) in CH_2Cl_2 at room temperature afforded homodinuclear complexes $[(Cp^*MCl)(4\text{-NSpy})(Cp^*MCl_2)]Cl$ [M = Rh (**8a**), Ir (**8b**)] in 67 and 72 % yields (Scheme 4), respectively. Complexes **8a**,**b** were also synthesized by reactions of $[Cp^*MCl_2]_2$ (M = Rh, Ir) with 1 equiv. of 4-NSpy (**1b**) in high yields. Heterodinulear complex $[(Cp^*IrCl)(4\text{-NSpy})(Cp^*RhCl_2)]Cl$ (**8d**) was prepared by reaction of **7b** with 0.5 equiv. of $[Cp^*RhCl_2]_2$ in CH_2Cl_2 at room temperature in 71 % yield. However, when similar reaction conditions were applied for the synthesis of $[(Cp^*RhCl)(4\text{-NSpy})(Cp^*IrCl_2)]Cl$ (**8c**), a mixture of **8a**–**d** was obtained, and hence, the reaction of **7a** with 0.5 equiv. of $[Cp^*IrCl_2]_2$ was carried out at –78 °C to give **8c** in a high yield of 71 %. The crystal structures of **8a**–**d** are essentially identical and a perspective plot for the complex cation of **8c** is illustrated in Figure 4 (those of **8a**,**b**,**d** are shown in Figures S3–S5, Supporting Information). The complex cations consist of two metal centers, Cp*M1Cl chelated by SN donors and Cp^*M2Cl_2 coordinated by a pyridyl nitrogen. The structure around the M1 atom is the same as in **7** [M1–Cl1 2.403(3)–2.419(2) Å, M1–S1 2.339(2)–2.373(1) Å, M1–N1 2.127(3)–2.135(8) Å]. The arrangement of the $Cp^*M_2Cl_2$ fragment in **8a**,**c** differs from that in **8b**,**d** in terms of the relationship of the two Cp* rings; two Cp* rings in **8a**,**c** are almost parallel, whereas those in **8b**,**d** are perpendicular [dihedral angle of two Cp* rings: 9.5(2)° (**8a**), 59.4(3)° (**8b**), 11.78(4)° (**8c**), 76.7(6)° (**8d**)]. In the ^{1}H NMR spectra of **8a**–**d** in CD_3OD, two singlet peaks attributable to two Cp* rings were observed; the peaks for the Cp* ring on M1 center (SN site) appeared at δ = 1.62 (**8a**), 1.60 (**8b**), 1.59 (**8c**), 1.60 (**8d**) ppm, whereas the peaks for the Cp* ring on M2 center (py site) are slightly shifted depending on M ion at 1.59 (**8a**), 1.55 (**8b**), 1.54 (**8c**), 1.58 (**8d**) ppm (Figure 5). These assignments are supported by ^{1}H NMR spectra of **9** and **10** (vide infra). Complexes **8a**, **8b**, and **8d** are stable at room temperature in solution, whereas heterodinuclear complex **8c** is unstable at room temperature; this species gives a mixture of **8a**–**d** via the SN and py site exchange reactions of Cp*M fragments, which will be discussed in detail (vide infra).

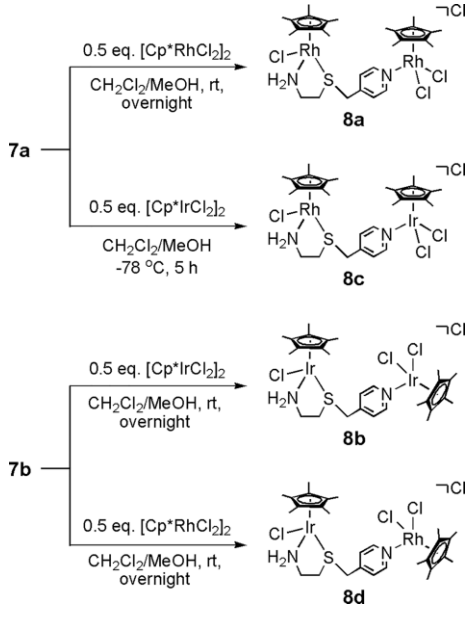

Scheme 4. Preparations of homo- and heterodinuclear complexes, $[(Cp^*MCl)(4\text{-NSpy})(Cp^*M'Cl_2)]Cl$ [M, M′ = Rh, Rh (**8a**); Ir, Ir (**8b**); Rh, Ir (**8c**); Ir, Rh (**8d**)].

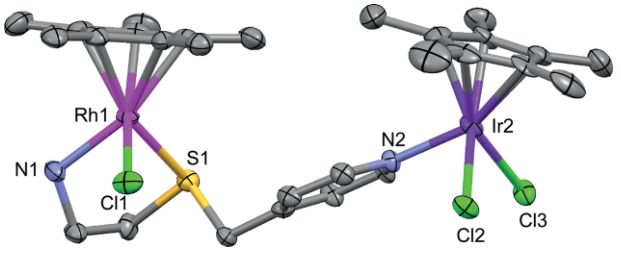

Figure 4. ORTEP diagram for the complex cation of **8c** with the atomic numbering scheme. The thermal ellipsoids are drawn at the 40 % probability level, and the hydrogen atoms are omitted for clarity.

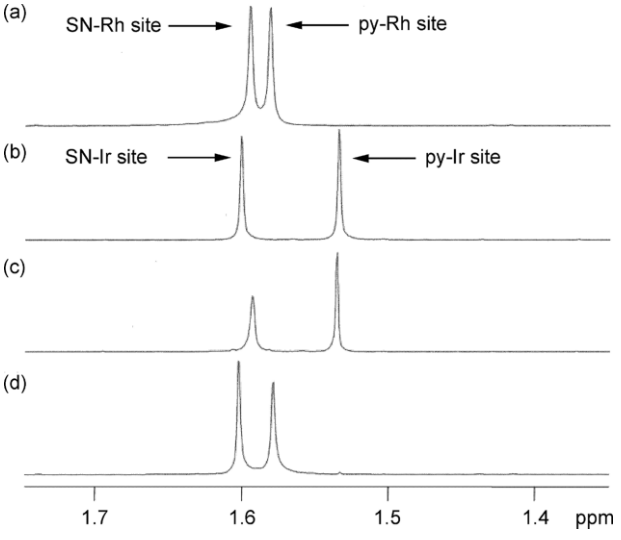

Figure 5. ^{1}H NMR spectra for the Cp* region of (a) **8a**, (b) **8b**, (c) **8c**, and (d) **8d** in CD_3OD at room temperature.

With the aim of understanding SN and py site selectivities of Cp*M (M = Rh, Ir) fragments, appropriate mononuclear model complexes [(Cp*MCl)(NSph)]Cl [M = Rh (**9a**), Ir (**9b**)] and [(Cp*MCl)(4-Mepy)]Cl [M = Rh (**10a**), Ir (**10b**)] were synthesized by reacting $[Cp^*MCl_2]_2$ (M = Rh, Ir) with 2 equiv. of 2-(benzylthio)ethanamine (NSph) or 4-methylpyridine (4-Mepy) in CH_2Cl_2 (Scheme 5). The structures of **9a**,**b** were determined by X-ray crystallography to be similar to those of **7a**,**b**, in which 4-pyridyl substituents were replaced by phenyl groups and indicate that configuration around the M1 and sulfur centers are the same

as those observed in **7** and **8** (Figures S6 and S7, Supporting Information). The ^{1}H NMR spectra of **9** in CD_3OD exhibited a singlet peak for Cp* ring at δ = 1.58 (**9a**), 1.59 ppm (**9b**) and the ESI-MS spectra of **9** in CH_3OH showed an intense monovalent peak for $[(Cp^*MCl)(NSph)]^+$ at 440.11 (**9a**) and 530.19 (**9b**). The structures of **10a** and **10b** are isomorphous consisting of a Cp^*MCl_2 center coordinated by the pyridyl nitrogen atom of 4-Mepy [M1–N1 2.056(2) Å (**10a**), 2.121(5) Å (**10b**)]. A singlet peak for the Cp* ring was observed at δ = 1.56 ppm (**10a**) and 1.51 ppm (**10b**), and the coordination of 4-Mepy in solution was confirmed by the lower field shift of a doublet peak for the pyridyl 2,6-aromatic protons with respect to non-coordinated 4-Mepy [δ = 8.79 (**10a**), 8.76 ppm (**10b**)] in the ^{1}H NMR spectra.

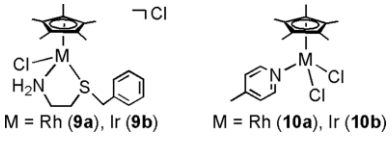

Scheme 5. Structures of [(Cp*MCl)(NSph)]Cl (**9**) and [(Cp*MCl)(4-Mepy)]Cl (**10**) [M, M′ = Rh (**a**), Ir (**b**)].

The four competitive reactions, (a) 1 equiv. $[Cp^*RhCl_2]_2$ + 1 equiv. $[Cp^*IrCl_2]_2$ + 2 equiv. NSph, (b) 1 equiv. $[Cp^*RhCl_2]_2$ + 1 equiv. $[Cp^*IrCl_2]_2$ + 2 equiv. 4-Mepy, (c) 1 equiv. $[Cp^*IrCl_2]_2$ + 2 equiv. NSph + 2 equiv. 4-Mepy, and (d) 1 equiv. $[Cp^*RhCl_2]_2$ + 1 equiv. $[Cp^*IrCl_2]_2$ + 2 equiv. NSph + 2 equiv. 4-Mepy in $CDCl_3$ were carried out to investigate metal selectivity for each ligand. The reactions (a)–(c) led to selective formation of **9b** (a), **10b** (b), **9b** (c) in quantitative yields as confirmed by the ^{1}H NMR spectra (Scheme 6). High selectivity of iridium(III) ion for these ligands in reactions (a) and (b) can be explained by the stronger ligand field of iridium(III) ion relative to rhodium(III).[12] Reaction (d) provided a mixture of all dinuclear complexes of **9a**, **9b**, **10a**, and **10c** with a ratio of 18:82:82:18. In addition, two reactions of (e) 1 equiv. **9a** + 1 equiv. **10b** and (f) 1 equiv. **9b** + 1 equiv. **10a** in $CDCl_3$ at room temperature were examined as model systems for coordination-site-exchange reactions of **8c** and **8d**; both reactions (e) and (f) afforded mixtures of **9a**, **9b**, **10a**, and **10b** in the same ratio as had been found for reaction (d).

The site exchange reaction of **8c** was monitored by ^{1}H NMR spectroscopy in CD_3OD at 55 °C and ultimately afforded four singlet peaks at δ = 1.59, 1.60, 1.58, and 1.53 ppm assignable to four different Cp* rings of Cp*Rh(SN), Cp*Ir(SN), Cp*Rh(py), and Cp*Ir(py) in a ratio of 16:84:84:16 (Figure 6), in good agreement with the results of reactions (e) and (f). The ratio of **8a**–**d** was estimated from the final ^{1}H NMR spectral ratio to be 13:13:3:71. Although complex **8d** was quite stable at room temperature, warming the solution at 55 °C for 1 d resulted in a mixture of **8a**–**d** in the same ratio as had been identified with **8c**. Formation of homodinuclear complexes **8a** and **8b** from site-exchange reactions of heterodinuclear complexes **8c** or **8d** indicates that intermolecular exchange reactions of Cp*M units are involved in the scrambling reaction (Scheme 7). To confirm this assertion, a mixture of homodinuclear complexes **8a** and **8b** in CD_3OD was heated at 55 °C and monitored by ^{1}H NMR spectroscopy. A similar site exchange reaction was noted during these studies and this exchanged ultimately, reached an equilibrium mixture of **8a**–**d** in the same ratio as had been noted previously from **8c** and **8d** (Figure S12, Supporting Information). Although there are several examples of mixed-metal dinuclear complexes containing Cp*Rh and Cp*Ir fragments,[13] intermolecular exchange reactions have not been previously mentioned except for our previous report on the stepwise synthesis of heterotrinuclear complexes with Pd, Rh, and Ir ions assembled by a tetraphosphine ligand.[3q] Consequently, the coordination-site-exchange reactions of **8** might constitute an important ex-

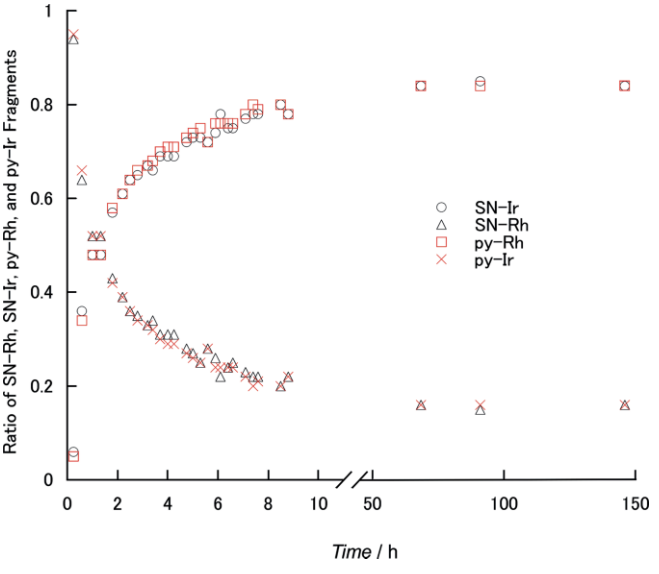

Figure 6. Ratios of SN-Rh, SN-Ir, py-Rh, and py-Ir fragments vs. time as obtained by heating **8c** in CD_3OD at 55 °C.

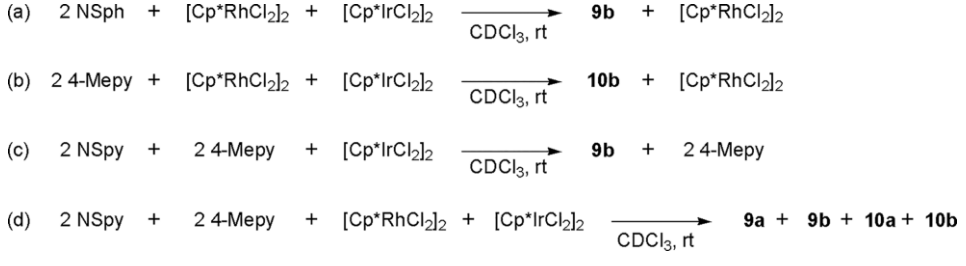

Scheme 6. Competitive reactions to investigate metal selectivity between SN and py sites.

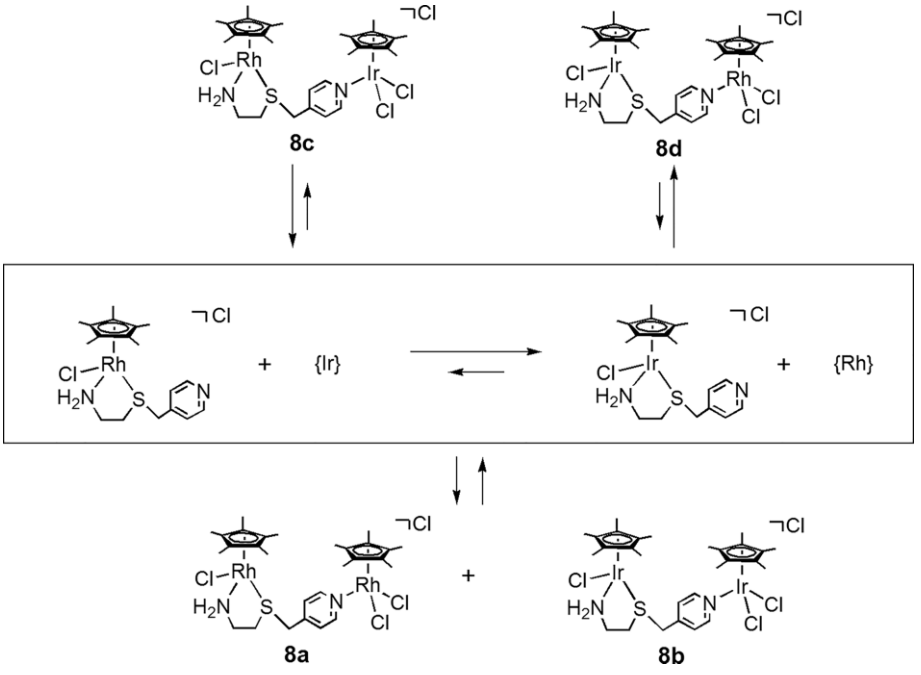

Scheme 7. Coordination-site-exchange reactions of Cp*M units between **8a**–**d**; {M} = Cp^*MCl_2.

ample of how to scrutinize differences in coordination behaviors between the Cp*Rh and Cp*Ir fragments.

Conclusions

In the present study, homodinuclear Cp^*Rh^{III} and Cp^*Ir^{III} complexes, $[(Cp^*MCl)(2\text{-pyNSpy})(Cp^*MCl)](PF_6)_2$ [M = Rh (**5a**), Ir (**5b**)], $[(Cp^*M)(2\text{-py}_2\text{NSpy})(Cp^*MCl)](PF_6)_3$ [M = Rh (**6a**), Ir (**6b**)], and $[(Cp^*MCl)(4\text{-NSpy})(Cp^*MCl_2)]Cl$ [M = Rh (**8a**), Ir (**8b**)] were synthesized using a series of SN_n mixed-donor ligands. Heterodinuclear complexes $[(Cp^*MCl)(4\text{-NSpy})(Cp^*M'Cl_2)]Cl$ [M, M′ = Rh, Ir (**8c**), Ir, Rh (**8d**)] were also prepared by the reactions of mononuclear complexes [(Cp*MCl)(4-NSpy)]Cl [M = Rh (**7a**), Ir (**7b**)] with $[Cp^*MCl_2]_2$ (M = Ir, Rh). Configurations around the Cp*MCl metal centers coordinated by $2\text{-pyCH}_2\text{SR}$ and $H_2NC_2H_4SR$ moieties were regulated by the configuration of sulfur atoms leading to selective formation of R_MR_S/S_MS_S isomers in **6**–**8**, which are retained in solution. On the other hand, the configuration of the secondary amine nitrogen atom of the $2\text{-pyCH}_2\text{NHR}$ residue is likely to be racemized to afford four possible diastereomers of **5**. Heterodinuclear complexes **8c**,**d** are unstable in solution and give a mixture of **8a**–**d** via coordination-site-exchange of Cp*M fragments, which is promoted by the stronger binding affinity of iridium(III) ion for the SN and py sites relative to rhodium(III) ion.

Experimental Section

General: All manipulations were carried out under a nitrogen atmosphere using standard Schlenk techniques. 2-[(2-Pyridinyl)methylthio]ethanamine (2-NSpy, **1a**) and 2-[(4-pyridinyl)methylthio]ethanamine (4-NSpy, **1b**) were prepared by the reported procedures.[9] Reagent grade solvents were dried by the standard procedures and were freshly distilled prior to use. IR spectra were recorded using a Jasco FT/IR-410 spectrophotometer. ^1H and $^{13}C\{^1H\}$ NMR spectra were recorded with a JEOL JMN-AL400 spectrometer at 400 and 100 MHz, respectively, and were referenced to TMS as the external standard. ESI-TOF MS spectra were recorded with a JEOL JMS-T100LC high-resolution mass spectrometer using positive ionization mode.

2-(2-Pyridinyl)methylthio-*N*-(2-pyridinylmethyl)ethanamine (2-pyNSpy) (2): To a solution of **1a** (3.4 g, 20 mmol) in MeOH (200 mL) was added 2-pyridinealdehyde (2.1 g, 20 mmol). After the solution was stirred at room temp. for 2 h, $NaBH_4$ (0.75 g, 20 mmol) was added by several portions and the resulting solution was stirred at room temp. for 1 h. The solvent was removed under reduced pressure. The residue was extracted with $CHCl_3$ and washed with water. The organic phase was dried with Na_2SO_4. After filtration, the solvent was removed under reduced pressure to afford pale brown oil **2** (91 %, 4.7 g). IR (nujor): $\tilde{\nu}$ = 3303 (br), 2921 (m), 2851 (m), 1591 (s), 1569 (m), 1473 (m), 1434 (s), 1123 (w), 994 (w), 751 (m) cm^{-1}. ^1H NMR (400 MHz, $CDCl_3$): δ = 8.52 (d, ^3J = 5 Hz, 1 H), 8.48 (d, ^3J = 5 Hz, 1 H), 7.61 (dt, ^3J = 8, ^4J = 2 Hz), 7.33 (d, ^3J = 8 Hz, 1 H), 7.28 (d, ^3J = 8 Hz, 1 H), 7.14 (t, ^3J = 4 Hz, 1 H), 7.12 (t, ^3J = 4 Hz, 1 H), 3.88 (s, 2 H), 3.82 (s, 2 H), 2.83 (t, ^3J = 6 Hz, 2 H), 2.69 (t, ^3J = 6 Hz, 2 H), 2.41 (br., 2 H) ppm. ^{13}C NMR (100 MHz, $CDCl_3$): δ = 159.4, 158.6, 149.1, 149.0, 136.5, 136.2, 122.9, 122.0, 121.74, 121.72, 54.8, 48.0, 37.9, 32.0 ppm.

2-(2-Pyridinyl)methylthio-*N*,*N*-bis[(2-pyridinyl)methyl]ethanamine (2-py$_2$NSpy, 3): To a solution of 2-(chloromethyl)pyridine hydrochloride (0.16 g, 0.10 mmol) in EtOH (10 mL) was added **2** (0.26 g, 0.10 mmol) and $NaHCO_3$ (0.84 g, 10 mmol). After the mixture was stirred at 60 °C for 6 d, the resultant solution was filtered and dried in vacuo. The residue was extracted with $CHCl_3$ and washed with water. The organic phase was dried with Na_2SO_4. After filtration, the solvent was removed under reduced pressure and the crude product was purified with silica gel column chromatography ($CHCl_3$/MeOH = 95:5) to give dark brown oil **3** (73 %, 2.5 g). IR (nujor): $\tilde{\nu}$ = 3390 (br), 2924 (m), 2853 (m), 1590 (s), 1569 (s), 1471 (m),

1434 (s), 1377 (s), 1304 (m), 1148 (w), 994 (m), 761 (s) cm^{-1}. ^1H NMR (400 MHz, $CDCl_3$): δ = 8.47–8.44 (m, 3 H), 7.63–7.50 (m, 5 H), 7.26 (s, 1 H), 7.12–7.08 (m, 3 H), 3.78 (s, 4 H), 3.74 (s, 2 H), 2.77–2.72 (m, 2 H), 2.68–2.64 (m, 2 H) ppm. ^{13}C NMR (100 MHz, $CDCl_3$): δ = 159.2, 158.5, 149.0, 148.7, 136.5, 136.3, 122.8, 122.8, 121.8, 121.7, 60.1, 53.6, 38.2, 29.3 ppm.

2-(Benzylthio)ethanamine (NSph, 4): To a solution of cysteamine hydrochloride (3.4 g, 30 mmo) in EtOH (30 mL) was added benzylchloride (2.5 g, 20 mmol) and $NaHCO_3$ (16.9 g, 201 mmol). After stirring at room temp. for 2 d, the resultant solution was filtered and dried in vacuo. The residue was extracted with $CHCl_3$ and washed with water. The organic phase was dried with Na_2SO_4. After filtration, the solvent was removed under reduced pressure to afford pale orange oil **4** (76 %, 2.4 g). ^1H NMR (400 MHz, $CDCl_3$): δ = 7.25 (m, 5 H, Ar), 3.64 (s, 2 H), 2.75 (t, ^3J = 6 Hz, 2 H), 2.46 (t, ^3J = 6 Hz, 2 H), 1.33 (br., 2 H, NH_2) ppm. ^{13}C NMR (100 MHz, $CDCl_3$): δ = 138.2, 128.6, 128.3, 126.8, 40.9, 36.0, 35.6 ppm.

[(Cp*RhCl)$_2$(2-pyNSpy)](PF$_6$)$_2$ (5a): To a solution of $[Cp^*RhCl_2]_2$ (40 mg, 0.065 mmol) in CH_2Cl_2 (5 mL) was added **2** (17 mg, 0.065 mmol), NH_4PF_6 (21 mg, 0.13 mmol), and MeOH (5 mL) and the resulting mixture was stirred at room temp. overnight. The solvent was removed under reduced pressure to dryness, and the residue was extracted with CH_2Cl_2, to which hexane was carefully added. This mixture was allowed to stand in the refrigerator to afford red crystals of **5a**·0.5CH_2Cl_2 (86 %, 62 mg). $C_{34.5}H_{48}Cl_3F_{12}N_3P_2Rh_2S$ (**5a**·0.5CH_2Cl_2, 1138.93): calcd. C 36.38, H 4.25, N 3.69; found C 36.67, H 4.43, N 3.81. IR (KBr): $\tilde{\nu}$ = 3646 (w), 3464 (br), 3299 (w), 2970 (w), 2923 (w), 1608 (m), 1452 (m), 1381 (m), 1271 (w), 1162 (w), 1028 (m), 841 (s), 577 (s) cm^{-1}. UV/Vis (MeCN): λ_{max} (ε, L mol^{-1} cm^{-1}) = 241 (50000), 377 (7600) nm. ^1H NMR (400 MHz, CD_3CN): δ = 8.63–8.44 (m, 2 H, py), 8.04–7.94 (m, 2 H, py), 7.66–7.47 (m, 4 H, py), 4.50–3.95 (m, 4 H), 3.01–2.73 (m, 3 H), 2.48–2.43 (m, 1 H), 2.28 (br), 1.70, 1.69, 1.67, 1.66, 1.63, 1.57, 1.56, 1.46 (s, 30 H, CH_3) ppm. ^{13}C NMR (100 MHz, CD_3CN): δ = 160.1, 160.0, 159.9, 159.2, 155.0, 154.8, 154.1, 153.0, 152.7, 152.7, 141.0, 140.7, 140.6, 140.3, 127.8, 127.4, 127.0, 126.9, 126.7, 126.1, 125.7, 123.8, 123.7, 100.8–100.5, 97.4–97.2 (m, Cp*ring), 61.3, 60.5, 59.7, 51.9, 51.6, 49.8, 45.2, 45.2, 45.1, 34.6, 32.9, 32.4 (aliphatic), 9.77, 9.63, 9.55, 9.38 (Cp*CH_3) ppm. ESI-MS (in MeCN): m/z = 949.83 (z1, {[Cp*$_2$Rh$_2$Cl$_2$(2-pyNSpy)](PF$_6$)}$^+$ (calcd. 950.06)), 580.80 (z1, {Cp*$_2$Rh$_2$Cl$_3$}$^+$ (calcd. 580.95)).

[(Cp*IrCl)$_2$(2-pyNSpy)](PF$_6$)$_2$ (5b): By a procedure similar to that for **5a**, using $[Cp^*IrCl_2]_2$ (50 mg, 0.065 mmol), **2** (16 mmg, 0.065 mmol), and NH_4PF_6 (21 mg, 0.13 mmol), red crystals of **5b**·0.5CH_2Cl_2 (53 %, 42 mg) were isolated. $C_{34.5}H_{48}Cl_3F_{12}Ir_2N_3P_2S$ (**5b**·0.5CH_2Cl_2, 1317.56): calcd. C 31.45, H 3.67, N 3.19, S 2.43; found C 31.51, H 3.55, N 3.35, S 2.41. UV/Vis (MeCN): λ_{max} (ε, L mol^{-1} cm^{-1}) = 265 (11000), 306 (6100) nm. IR (KBr): $\tilde{\nu}$ = 3292 (w), 2979 (w), 2925 (w), 1611 (m), 1455 (m), 1387 (m), 1035 (m), 844 (s), 768 (m), 557 (s) cm^{-1}. ^1H NMR (400 MHz, CD_3CN): δ = 8.64–8.45 (m, 2 H, py), 8.05–7.96 (m, 2 H, py), 7.80–7.49 (m, 4 H, py), 6.02 (br), 5.89 (br), 5.76 (br), 5.56 (br), 4.66–4.02 (m, 4 H), 3.45–2.49 (m, 3 H), 1.73, 1.70, 1.69, 1.67, 1.64, 1.55, 1.53, 1.46 (s, 30 H, CH_3) ppm. ESI-MS (in CH_3CN): m/z = 1130.28 (z1, {[Cp*$_2$Ir$_2$Cl$_2$(2-pyNSpy)](PF$_6$)}$^+$ (calcd. 1130.17)), 1094.29 (z1, {[Cp*$_2$Ir$_2$Cl(2-pyNSpy)](PF$_6$)$_2$-H}$^+$ (calcd. 1094.20)).

[Cp*$_2$Rh$_2$Cl(2-py$_2$NSpy)](PF$_6$)$_3$ (6a): To a solution of $[Cp^*RhCl_2]_2$ (50 mg, 0.081 mmol) in CH_2Cl_2 (5 mL) was added **3** (28 mg, 0.079 mmol), NH_4PF_6 (40 mg, 0.24 mmol), and MeOH (5 mL) and the resulting mixture was stirred at room temp. overnight. The solvent was removed under reduced pressure to dryness, and the residue was extracted with CH_2Cl_2. The extract was concentrate to form yellow precipitate, which was recovered by filtration and crystallized from MeCN/Et_2O to afford orange crystals of **6a**·0.5MeCN (36 %, 38 mg). $C_{41}H_{53.5}ClF_{18}N_{4.5}P_3Rh_2S$ (**6a**·0.5CH_3CN, 1317.62): calcd. C 37.37, H 4.09, N 4.78; found C 37.28, H 4.10, N 5.16. IR (KBr): $\tilde{\nu}$ = 3653 (w), 3435 (br), 1610 (m), 1487 (m), 1448 (m), 1165 (w), 1026 (m), 841 (s), 769 (m), 559 (s) cm^{-1}. UV/Vis (MeCN): λ_{max} (ε, L mol^{-1} cm^{-1}) = 236 (44000), 334 (5100) nm. ^1H NMR (400 MHz, CD_3CN): δ = 8.65 (d, ^3J = 4 Hz, 1 H), 8.55 (d, ^3J = 6 Hz, 1 H), 8.45 (d, ^3J = 5 Hz, 1 H), 8.09 (dt, ^3J = 8, ^4J = 1 Hz, 1 H), 7.95–7.88 (m, 2 H), 7.75 (d, ^3J = 8 Hz, 1 H), 7.62 (t, ^3J = 6 Hz, 1 H), 7.56 (t, ^3J = 6 Hz, 1 H), 7.50 (t, ^3J = 6 Hz, 1 H), 7.33 (d, ^3J = 9 Hz, 2 H), 7.31 (d, ^3J = 9 Hz, 2 H), 4.63–4.24 (m, 4 H), 4.22 (d, ^2J = 16 Hz, 1 H), 4.04 (d, ^2J = 17 Hz, 1 H), 3.95 (dt, ^2J = 13, ^3J = 6 Hz, 1 H), 3.77 (dt, ^2J = 12, ^3J = 4 Hz, 1 H), 3.16–3.01 (m, 2 H), 1.72 (s, 15 H, Cp*), 1.64 (s, 15 H, Cp*) ppm. ^{13}C NMR (100 MHz, CD_3CN): δ = 161.0, 160.0, 159.8, 155.3, 152.2, 151.9, 142.0, 141.9, 141.8, 128.7, 128.4, 127.7, 126.4, 125.2, 124.4, 101.4 (d, J_{CRh} = 7 Hz), 100.6 (d, J_{CRh} = 8 Hz), 68.2, 66.8, 62.4, 47.9, 30.2, 10.1, 9.9 ppm. ESI-MS (CH_3CN): m/z = 1151.34 (z1, {[Cp*$_2$Rh$_2$Cl(2-pyNSpy$_2$)](PF$_6$)$_2$}$^+$ (calcd. 1151.09)), 1005.34 (z1, {[Cp*$_2$Rh$_2$Cl(2-pyNSpy$_2$)](PF$_6$) – H}$^+$ (calcd. 1005.09)), 587.30 (z1, {[Cp*$_2$Rh(2-pyNSpy$_2$)]}$^+$ (calcd. 587.17)).

[Cp*$_2$Ir$_2$Cl(2-py$_2$NSpy)](PF$_6$)$_3$ (6b): By a procedure similar to that for **6a**, using $[Cp^*IrCl_2]_2$ (100 mg, 0.125 mmol), **2** (44 mmg, 0.13 mmol), and NH_4PF_6 (61 mg, 0.38 mmol), red crystals of **6b** (61 %, 114 mg) were isolated. $C_{40}H_{52}ClF_{18}Ir_2N_4P_3S$ (1475.71): calcd. C 32.56, H 3.55, N 3.80; found C 32.31, H 3.37, N 4.09. IR (KBr): $\tilde{\nu}$ = 3653 (w), 3431 (br), 1612 (m), 1487 (m), 1452 (m), 1165 (w), 1032 (m), 839 (s), 768 (m), 559 (s) cm^{-1}. UV/Vis (in MeCN): λ_{max} (ε, L mol^{-1} cm^{-1}) = 266 (36000), 304 (16000) nm. ^1H NMR (400 MHz, CD_3CN): δ = 8.67 (dd, ^3J = 6, ^4J = 1 Hz, 1 H), 8.54 (d, ^3J = 5 Hz, 1 H), 8.45 (d, ^3J = 5 Hz, 1 H), 8.11 (dt, ^3J = 8, ^4J = 2 Hz, 1 H), 7.97–7.86 (m, 3 H), 7.58 (t, ^3J = 7 Hz, 1 H), 7.52–7.42 (m, 4 H), 4.71 (d, ^2J = 19 Hz, 2 H), 4.52 (d, ^3J = 3 Hz, 2 H), 4.31 (q, ^2J = 10 Hz, 2 H), 4.00 (dt, ^2J = 12, ^3J = 5 Hz, 1 H), 3.83 (dt, ^2J = 12, ^3J = 4 Hz, 1 H), 3.32 (sex, ^3J = 6 Hz, 1 H), 3.15 (dt, ^2J = 10, ^3J = 4 Hz, 1 H), 1.72 (s, 15 H, Cp*), 1.59 (s, 15 H, Cp*) ppm. ^{13}C NMR (100 MHz, CD_3CN): δ = 161.6, 160.1, 159.5, 154.9, 151.2, 150.9, 141.6, 141.5, 141.4, 128.4, 128.1, 127.5, 125.3, 124.5, 123.7, 93.7, 92.0, 70.0, 68.5, 63.9, 49.5, 28.9, 9.0, 8.9 ppm. ESI-MS (in MeCN): m/z = 1331.25 (z1, {[Cp*$_2$Ir$_2$Cl(2-py$_2$NSpy)](PF$_6$)$_2$}$^+$ (calcd. 1331.21)), 1185.29 (z1, {[Cp*$_2$Ir$_2$Cl(2-py$_2$NSpy)](PF$_6$) – H}$^+$ (calcd. 1185.24)).

[(Cp*RhCl)(4-NSpy)]Cl (7a): To a solution of $[Cp^*RhCl_2]_2$ (100 mg, 0.16 mmol) in CH_2Cl_2 (5 mL) was added **1b** (82 mg, 0.49 mmol) and the resulting mixture was stirred at room temp. overnight. The solvent was removed under reduced pressure to dryness, and the residue was extracted with MeOH, to which Et_2O was carefully added. This mixture was allowed to stand in the refrigerator to afford red crystals of **7a** (78 %, 120 mg). $C_{18}H_{27}Cl_2N_2RhS$ (477.30): calcd. C 45.30, H 5.70, N 5.87; found C 45.22, H 5.27, N 5.93. IR (KBr): $\tilde{\nu}$ = 3167 (m), 3063 (s), 2954 (s), 1599 (s, py), 1589 (m), 1413 (m), 1376 (m, Cp*), 1028 (m, Cp*), 993 (m) cm^{-1}. UV/Vis (MeOH): λ_{max} (ε, L mol^{-1} cm^{-1}) = 372 (3000), 269 (7400), 246 (1.8 × 10^4) nm. ^1H NMR (400 MHz, CD_3OD): δ = 8.57 (d, ^3J = 4 Hz, 2 H), 7.66 (d, ^3J = 4 Hz, 2 H), 4.63 (d, ^2J = 11 Hz, 1 H), 3.97 (dd, ^2J = 11, ^4J = 1 Hz, 1 H), 3.11–3.07 (m, 1 H), 2.97–2.87 (m, 2 H), 2.72–2.65 (m, 1 H), 1.62 (s, 15 H, CH_3) ppm. ^{13}C NMR (100 MHz, CD_3OD): δ = 150.4, 145.7, 127.1 (d, J_{CRh} = 4 Hz, py), 99.7 (d, J_{CRh} = 7 Hz), 45.1, 38.9, 36.7, 9.14 (d, J_{CRh} = 3 Hz) ppm. ESI-MS (MeOH): m/z = 441.14 (z1, [RhCp*Cl(4-NSpy)]$^+$ (calcd. 441.07)).

[(Cp*IrCl)(4-NSpy)]Cl (7b): By a procedure similar to that for **7a**, using $[Cp^*IrCl_2]_2$ (50 mg, 0.063 mmol) and **1b** (63 mmg, 0.38 mmol), red crystals of **7b** (81 %, 58 mg) were isolated. $C_{18}H_{27}Cl_2IrN_2S$

(566.61): calcd. C 38.16, H 4.80, N 4.94, S 5.66; found C 37.88, H 4.68, N 5.04, S 5.48. IR (KBr): $\tilde{\nu}$ = 3041 (s), 2959 (s), 2917 (s), 1599 (s), 1590 (m), 1455 (m), 1413 (m), 1177 (m), 998 (m) cm^{-1}. UV/Vis (MeOH): λ_{max} (ε, L mol^{-1} cm^{-1}) = 263 (4900), 332 (1700), 407 (320) nm. ^1H NMR (400 MHz, CD_3OD): δ = 8.56 (dd, ^3J = 4, ^4J = 2 Hz, 2 H), 7.64 (dd, ^3J = 4, ^4J = 2 Hz, 2 H), 4.84 (d, J = 11 Hz, 1 H), 3.93 (d, J = 12 Hz, 1 H), 3.05–2.90 (m, 3 H), 2.65–2.57 (m, 1 H), 1.62 (s, 15 H, CH_3) ppm. ^{13}C NMR (100 MHz, CD_3OD): δ = 150.4, 145.5, 127.2, 92.5, 46.0, 40.2, 34.9, 8.7 ppm. ESI-MS (in MeOH): m/z = 531.20 {z1, $[Cp^*IrCl(4\text{-}NSpy)]^+$ (calcd. 531.12)}.

[(Cp*RhCl)(Cp*RhCl$_2$)(4-NSpy)]Cl (8a): From **1b**: To a solution of $[Cp^*RhCl_2]_2$ (100 mg, 0.16 mmol) in CH_2Cl_2 (5 mL) was added **1b** (27 mg, 0.16 mmol). After the resulting mixture was stirred at room temp. overnight, hexane was carefully added. This mixture was allowed to stand in the refrigerator to afford red crystals of **8a**·0.25CH_2Cl_2 (82 %, 104 mg). From **7a**: To a solution of **7a** (30 mg, 0.063 mmol) in MeOH (5 mL) was added $[Cp^*RhCl_2]_2$ (19 mg, 0.031 mmol) in CH_2Cl_2 (5 mL) and the resulting mixture was stirred at room temp. overnight. The solvent was removed under reduced pressure to dryness, and the residue was extracted with CH_2Cl_2, to which Et_2O was carefully added. This mixture was allowed to stand in the refrigerator to afford red crystals of **8a**·0.5CH_2Cl_2 (67 %, 33 mg). $C_{28.25}H_{42.5}Cl_{4.5}N_2Rh_2S$ (**8a**·0.25CH_2Cl_2, 807.57): calcd. C 42.02, H 5.30, N 3.47, S 3.97; found C 41.96, H 5.41, N 3.51, S 3.95. IR (KBr): $\tilde{\nu}$ = 3386 (s), 3180 (s), 3056 (s), 2979 (s), 1611 (s, py), 1587 (m), 1452 (s), 1425 (s), 1375 (m, Cp*), 1027 (m, Cp*), 822 (m) cm^{-1}. UV/Vis (CH_2Cl_2): λ_{max} (ε, L mol^{-1} cm^{-1}) = 245 (10123), 271 (4165), 381 (1640) nm. ^1H NMR (400 MHz, CD_3OD): δ = 8.88 (d, J = 5 Hz, 2 H), 7.71 (d, J = 6 Hz, 2 H), 4.62 (d, J = 11 Hz, 1 H), 4.03 (d, J = 11 Hz, 1 H), 2.87 (dt, J = 13, J = 3 Hz, 2 H), 2.65 (dt, J = 13, J = 6 Hz, 2 H), 1.59 [s, 15 H, Cp*(SN-Rh site)], 1.58 [s, 15 H, Cp*(py-Rh site)] ppm. ^1H NMR (400 MHz, $CDCl_3$): δ = 8.91 (br. s, 2 H), 7.62 (d, ^3J = 5 Hz, 2 H), 4.60 (d, ^2J = 11 Hz, 1 H), 3.85 (d, ^2J = 11 Hz, 1 H), 3.37–3.27 (m, 2 H), 2.84–2.75 (m, 2 H), 1.62 [s, 15 H, Cp*(SN-Rh site)], 1.59 [s, 15 H, Cp*(py-Rh site)] ppm. ^{13}C NMR (100 MHz, CD_3OD): δ = 154.6, 147.5, 128.1, 99.9 (d, J_{CRh} = 8 Hz), 96.0 (d, J_{CRh} = 9 Hz), 45.1, 39.0, 36.2, 9.3 (CH_3), 9.1 (CH_3) ppm. ^{13}C NMR (100 MHz, $CDCl_3$): δ = 153.6, 145.2, 126.6, 99.1 (d, $^1J_{CRh}$ = 8 Hz), 94.0 (d, J_{CRh} = 9 Hz), 44.4, 38.5, 35.3, 9.6, 9.1 ppm. ESI-MS (MeOH): m/z = 751.06 {z1, [(Cp*RhCl)-(4-NSpy)(Cp*RhCl$_2$)]$^+$ (calcd. 751.02)}, 580.91 [z1, $(Cp^*_2Rh_2Cl_3)^+$ (calcd. 580.95)], 576.93 {z1, $[Cp^*_2Rh_2Cl_2(OMe)]^+$ (calcd. 577.00)}, 573.00 {z1, $[Cp^*_2Rh_2Cl(OMe)_2]^+$ (calcd. 573.06)}, 441.01 {z1, $[Cp^*RhCl(4\text{-}NSpy)]^+$ (calcd. 441.06)}.

[(Cp*IrCl)(Cp*IrCl$_2$)(4-NSpy)]Cl (8b): From **1b** by a procedure similar to that for **8a**, using $[Cp^*IrCl_2]_2$ (100 mg, 0.13 mmol) and **1b** (22 mmg, 0.13 mmol): red crystals of **8b**·0.5CH_2Cl_2 (73 %, 89 mg) were isolated. From **7b** by a procedure similar to that for **8a**, using $[Cp^*IrCl_2]_2$ (21 mg, 0.026 mmol) and **7b** (30 mmg, 0.53 mmol): red crystals of **8b**·0.5CH_2Cl_2 (72 %, 37 mg) were isolated. $C_{28.5}H_{43}Cl_5Ir_2N_2S$ (**8b**·0.5CH_2Cl_2, 1007.42): calcd. C 33.98, H 4.30, N 2.78, S 3.18; found C 33.70, H 4.43, N 2.92, S 3.03. IR (KBr): $\tilde{\nu}$ = 3574 (s), 3043 (s), 2973 (m), 2918 (m), 1612 (s), 1582 (m), 1455 (m), 1427 (s), 1388 (m), 1031 (m), 860 (m) cm^{-1}. UV/Vis (MeOH): λ_{max} (ε, L mol^{-1} cm^{-1}) = 285 (17378), 334 (9834) nm. ^1H NMR (400 MHz, CD_3OD): δ = 8.87 (d, J = 7 Hz, 2 H), 7.67 (d, J = 6 Hz, 2 H), 5.68 (br., 1 H), 5.54 (br., 1 H), 4.02 (d, J = 11 Hz, 1 H), 3.04–2.92 (m, 2 H), 2.58 (dt, J = 13, J = 5 Hz, 1 H), 1.60 [s, 15 H, Cp*(SN-Ir site)], 1.53 [s, 15 H, Cp*(py-Ir site)] ppm. ^1H NMR (400 MHz, $CDCl_3$): δ = 8.93 (d, J = 5 Hz, 2 H), 8.04 (br., 1 H), 7.54 (d, J = 6 Hz, 2 H), 4.87 (d, ^2J = 10 Hz, 1 H), 3.70 (d, ^2J = 10 Hz, 1 H), 3.54 (br., 1 H), 3.37 (br., 1 H), 2.83–2.71 (m, 2 H), 1.67 [s, 15 H, Cp*(SN-Ir site)], 1.55 [s, 15 H, Cp*(py-Ir site)] ppm. ^{13}C NMR (100 MHz, CD_3OD): δ = 154.7, 147.2, 128.4, 92.7, 87.4, 46.2, 40.4, 34.3, 8.9, 8.8 ppm. ^{13}C NMR (100 MHz, $CDCl_3$): δ = 153.5, 144.8, 126.7, 92.1, 85.8, 45.1, 40.0, 33.4, 9.2, 8.8 ppm. ESI-MS (in CH_3OH): m/z = 929.05 {z1, [(Cp*IrCl)(4-NSpy)(Cp*IrCl$_2$)]$^+$ (calcd. 929.14)}, 747.13 {z1, $[Cp^*_2Rh_2(OMe)_3]^+$ (calcd. 747.21)}, 531.06 {z1, $[(Cp^*IrCl)(4\text{-}NSpy)]^+$ (calcd. 531.12)}.

[(Cp*RhCl)(Cp*IrCl$_2$)(4-NSpy)]Cl (8c): To a solution of **7a** (30 mg, 0.063 mmol) in MeOH (5 mL) was added $[Cp^*IrCl_2]_2$ (25 mg, 0.031 mmol) in CH_2Cl_2 (5 mL) at –78 °C, and the resulting solution was stirred at –78 °C for 5 h. The solvent was removed under reduced pressure to dryness, and the residue was extracted with MeOH, to which Et_2O was carefully added. This mixture was allowed to stand in the refrigerator to afford red crystals of **8c**·CH_2Cl_2 (71 %, 42 mg). $C_{29}H_{44}Cl_6IrN_2RhS$ (**8c**·CH_2Cl_2, 960.58): calcd. C 36.26, H 4.62, N 2.92, S 3.34; found C 36.61, H 4.80, N 3.01, S 3.38. IR (KBr): $\tilde{\nu}$ = 3417 (m), 3066 (m), 2966 (m), 2920 (m), 1614 (m), 1454 (m), 1427 (m), 1380 (m), 1261 (w), 1028 (m) cm^{-1}. UV/Vis (MeOH): λ_{max} (ε, L mol^{-1} cm^{-1}) = 277 (14000), 368 (5300) nm. ^1H NMR (400 MHz, CD_3OD): δ = 8.88 (d, ^3J = 6 Hz, 2 H), 7.67 (d, ^3J = 6 Hz, 2 H), 4.69 (br., 1 H), 4.67 (d, ^2J = 11 Hz, 1 H), 4.06 (d, ^2J = 11 Hz, 1 H), 3.13 (br., 1 H), 3.01–2.89 (m, 2 H), 2.66 (dt, ^2J = 13, ^3J = 4 Hz, 1 H), 1.59 [s, 17 H, Cp*(SN-Rh site)], 1.54 [s, 15 H, Cp*(py-Ir site)] ppm. ^{13}C NMR (100 MHz, CD_3OD): δ = 154.7, 147.5, 128.4 (d, $^2J_{CRh}$ = 5 Hz), 99.9 (d, $^1J_{CRh}$ = 8 Hz), 87.4, 45.3, 39.0, 36.1, 9.3, 8.8 ppm. ESI-MS (in MeOH): m/z = 838.97 {z1, [(Cp*RhCl)(4-NSpy)(Cp*IrCl$_2$)]$^+$ (calcd. 839.08)}, 747.13 {z1, $[Cp^*_2Rh_2(OMe)_3]^+$ (calcd. 747.21)}, 441.00 {z1, $[Cp^*RhCl(4\text{-}NSpy)]^+$ (calcd. 441.06)}.

[(Cp*IrCl)(Cp*RhCl$_2$)(4-NSpy)]Cl (8d): To a solution of **7b** (30 mg, 0.063 mmol) in MeOH (5 mL) was added $[Cp^*RhCl_2]_2$ (17 mg, 0.027 mmol) in CH_2Cl_2 (5 mL), and the resulting solution was stirred at room temp. for 5 h. The solvent was removed under reduced pressure to dryness, and the residue was extracted with MeOH, to which Et_2O was carefully added. This mixture was allowed to stand in the refrigerator to afford red crystals of **8d** (90 %, 42 mg). $C_{28}H_{42}Cl_4IrN_2RhS$ (875.65): calcd. C 38.41, H 4.83, N 3.20, S 3.66; found C 38.29, H 4.74, N 3.24, S 3.50. IR (KBr): $\tilde{\nu}$ = 3460 (m), 3053 (s), 2968 (s), 2916 (m), 1608 (m), 1452 (m), 1425 (s), 1028 (m), 849 (w) cm^{-1}. UV/Vis (MeOH): λ_{max} (ε, L mol^{-1} cm^{-1}) = 247 (20000), 334 (2900), 395 (2700) nm. ^1H NMR (400 MHz, CD_3OD): δ = 8.87 (d, ^3J = 5 Hz, 2 H), 7.68 (d, ^3J = 7 Hz, 2 H), 5.65 (br., 1 H), 5.56 (br., 1 H), 4.84 (d, ^2J = 12 Hz, 1 H), 3.98 (d, ^2J = 11 Hz, 1 H), 3.01–2.91 (m, 3 H), 2.58 (dt, ^2J = 13, ^3J = 4 Hz, 1 H), 1.60 (s, 15 H, Cp*), 1.58 (s, 15 H, Cp*) ppm. ^{13}C NMR (100 MHz, CD_3OD): δ = 154.6, 147.2, 128.2, 96.0 (d, $^1J_{CRh}$ = 9 Hz), 92.7, 46.1, 40.4, 34.4, 9.1, 8.9 ppm. ESI-MS (in MeOH): m/z = 839.06 {z1, [(Cp*IrCl)(4-NSpy)(Cp*RhCl$_2$)]$^+$ (calcd. 839.08)}, 580.91 [z1, $(Cp^*_2Rh_2Cl_3)^+$ (calcd. 580.95)], 576.93 {z1, $[Cp^*_2Rh_2Cl_2(OMe)]^+$ (calcd. 577.00)}, 572.96 {z1, $[Cp^*_2Rh_2Cl(OMe)_2]^+$ (calcd. 573.06)}, 531.06 {z1, $[(Cp^*IrCl)(4\text{-}NSpy)]^+$ (calcd. 531.12)}.

[(Cp*RhCl)(NSph)]Cl (9a): To a solution of $[Cp^*RhCl_2]_2$ (100 mg, 0.16 mmol) in CH_2Cl_2 (10 mL) was added **4** (54 mg, 0.32 mmol). After the resulting mixture was stirred at room temp. overnight, hexane was carefully added. This mixture was allowed to stand in the refrigerator to afford orange crystals of **9a** (91 %, 141 mg). $C_{19}H_{28}Cl_2NRhS$ (476.31): calcd. C 47.91, H 5.93, N 2.94; found C 47.71, H 5.56, N 2.99. IR (KBr): $\tilde{\nu}$ = 3049 (br), 2958 (s), 1589 (s), 1493 (s), 1454 (s), 1377 (m), 1163 (m), 1030 (s), 995 (m), 764 (m), 706 (s) cm^{-1}. UV/Vis (MeOH): λ_{max} (ε, L mol^{-1} cm^{-1}) = 372 (2260), 279 (4050), 247 (12300) nm. ^1H NMR (400 MHz, CD_3OD): δ = 7.57 (dd, ^3J = 8, ^4J = 2 Hz, 2 H), 7.40–7.33 (m, 3 H), 4.63 (d, ^2J = 11 Hz, 1 H), 3.92 (dd, ^2J = 11, ^4J = 2 Hz, 1 H), 3.08–2.87 (m, 3 H), 2.62 (dt, ^2J = 13, ^4J = 4 Hz, 1 H), 1.58 (s, 15 H) ppm. ^1H NMR (400 MHz, $CDCl_3$): δ = 7.48 (dd, ^3J = 8, ^4J = 2 Hz, 2 H), 7.33–7.26 (m, 3 H), 4.57 (d, ^2J = 11 Hz, 1 H), 3.67 (dd, ^2J = 11, ^4J = 2 Hz, 1 H), 3.38–3.27 (m, 2 H), 2.89–2.81 (m, 1 H), 2.60 (d, ^2J = 15 Hz, 1 H), 1.64 (s, 15 H) ppm. ^{13}C

NMR (100 MHz, CD_3OD): δ = 135.2, 131.7, 129.7, 129.4, 99.5 (d, $^1J_{CRh}$ = 8 Hz), 45.6, 38.5, 38.3, 9.0 ppm. ^{13}C NMR (100 MHz, $CDCl_3$): δ = 133.2, 130.5, 128.6, 128.4, 98.4 (d, $^1J_{CRh}$ = 8 Hz), 44.6, 37.7, 37.6, 9.4 ppm. ESI-MS (in CH_3OH): *m/z* = 440.11 {*z*1, [Cp*RhCl(NSph)]$^+$ (calcd. 440.05)}.

[(Cp*IrCl)(NSph)]Cl (9b): By a procedure similar to that for **9a**, using $[Cp^*IrCl_2]_2$ (100 mg, 0.13 mmol) and **4** (84 mmg, 0.50 mmol), red crystals of **9b** (81 %, 116 mg) were isolated. $C_{19}H_{28}Cl_2IrNS$ (565.62): calcd. C 40.35, H 4.99, N 2.48, S 5.46; found C 39.97, H 5.02, N 2.51, S 5.46. IR (KBr): $\tilde{\nu}$ = 3033 (m), 2962 (s), 1589 (m), 1456 (s), 1324 (m), 1178 (m), 1038 (m), 860 (m), 760 (m), 704 (s) cm^{-1}. UV/Vis (MeOH): λ_{max} (ε, L mol^{-1} cm^{-1}) = 293 (2280), 340 (1040) nm. ^1H NMR (400 MHz, CD_3OD): δ = 7.55 (dd, ^3J = 8, ^4J = 2 Hz, 2 H), 7.39–7.32 (m, 3 H), 5.56 (br., 1 H), 4.81 (d, ^2J = 11 Hz, 1 H), 3.86 (d, ^2J = 11 Hz, 1 H), 3.02–2.95 (m, 2 H), 2.86 (dd, ^2J = 14, ^4J = 3 Hz, 1 H), 2.55 (dt, ^2J = 13, ^3J = 6 Hz, 1 H), 1.59 (s, 15 H, Cp*) ppm. ^1H NMR (400 MHz, $CDCl_3$): δ = 7.46 (dd, ^3J = 8, ^4J = 2 Hz, 2 H), 7.34–7.28 (m, 3 H), 4.72 (d, ^2J = 11 Hz, 1 H), 3.64 (d, ^2J = 11 Hz, 1 H), 3.52 (br), 3.35 (br), 3.22 (dt, ^2J = 13, ^4J = 4 Hz, 1 H), 2.93–2.84 (m, 1 H), 2.55 (d, ^2J = 12 Hz, 1 H), 1.90 (br), 1.67 (s, 15 H) ppm. ^{13}C NMR (100 MHz, CD_3OD): δ = 135.0, 131.7, 129.6, 129.3, 92.1, 46.6, 39.5, 36.8, 8.6 ppm. ^{13}C NMR (100 MHz, $CDCl_3$): δ = 132.9, 130.5, 128.6, 128.4, 91.3, 45.4, 38.9, 36.2, 9.0 ppm. ESI-MS (in CH_3OH): *m/z* = 530.19 {*z*1, [Cp*IrCl(NSph)]$^+$ (calcd. 530.13)}.

[(Cp*RhCl)(4-Mepy)]Cl (10a): To a solution of $[Cp^*RhCl_2]_2$ (50 mg, 0.081 mmol) in CH_2Cl_2 (5 mL) was added 4-methylpyridine (15 mg, 0.16 mmol). After the resulting mixture was stirred at room temp. for 2 d, Et_2O was carefully added. This mixture was allowed to stand in the refrigerator to afford orange crystals of **10a** (91 %, 141 mg). $C_{16}H_{22}Cl_2NRh$ (402.16): calcd. C 47.78, H 5.51, N 3.48; found C 47.62, H 5.45, N 3.46. IR (KBr): $\tilde{\nu}$ = 3431 (br), 3032 (w), 2963 (w), 2919 (w), 1617 (s), 1441 (s), 1375 (m), 1214 (s), 1029 (m), 814 (s) cm^{-1}. UV/Vis (CH_2Cl_2): λ_{max} (ε, L mol^{-1} cm^{-1}) = 405 (2900) nm. ^1H NMR (400 MHz, $CDCl_3$): δ = 8.79 (d, *J* = 5 Hz, 2 H), 7.15 (d, *J* = 6 Hz, 2 H), 2.39 (s, 3 H, CH_3), 1.56 (s, 15 H, Cp*CH_3) ppm. ^{13}C NMR (100 MHz, $CDCl_3$): δ = 152.6, 149.6, 126.1, 93.8 (d, $^1J_{C\text{-}Rh}$ = 9 Hz), 21.1, 9.0 ppm.

[(Cp*RhCl)(4-Mepy)]Cl (10b): By a procedure similar to that for **10a**, using $[Cp^*IrCl_2]_2$ (50 mg, 0.63 mmol) and 4-methylpyridine (12 mg, 0.13 mmol), red crystals of **10b** (62 %, 38 mg) were isolated. $C_{16}H_{22}Cl_2IrN$ (491.48): calcd. C 39.10, H 4.51, N 2.85; found C 38.93, H 4.31, N 2.83. IR (KBr): $\tilde{\nu}$ = 3441 (br), 3036 (w), 2964 (w), 2920 (w), 1618 (s), 1443 (s), 1381 (m), 1214 (s), 1028 (m), 816 (s) cm^{-1}. UV/Vis (CH_2Cl_2): λ_{max} (ε, L mol^{-1} cm^{-1}) = 267 (5400), 322 (3100), 427 (300) nm. ^1H NMR (400 MHz, $CDCl_3$): δ = 8.76 (d, *J* = 6 Hz, 2 H), 7.12 (d, *J* = 6 Hz, 2 H), 2.42 (s, 3 H), 1.51 (s, 15 H) ppm. ^{13}C NMR (100 MHz, $CDCl_3$): δ = 152.5, 149.6, 126.2, 85.5, 21.0, 8.7 ppm.

X-ray Crystallography: Crystals **5a**, **6a**, **6b**, **7a**, 7**b**, **8a**–**d**, **9a**, **9b**, **10a**, **10b** were quickly coated with Paratone N oil and mounted onto the top of a loop fiber at room temperature. Crystal and experimental data are summarized in Tables S1–S4 (Supporting Information). All data were collected at low temperature with a Rigaku VariMax Mo/Saturn CCD diffractometer equipped with graphite-monochromated confocal Mo-K_α radiation using a rotating-anode X-ray generator RA-Micro7 (50 kV, 24 mA: **7a**, **8a**, **8b**, **8b**, **8c**, **9a**, **9b**, **10a**, **10b**) and a Rigaku AFC8R/Mercury CCD diffractometer equipped with graphite-monochromated Mo-K_α radiation using a rotating-anode X-ray generator (44 kV, 200 mA: **5a**; 50 kV, 180 mA: **6a**, **8a**; 50 kV, 190 mA: **6b**, **7b**, **8d**). A total of 720 (**7a**, **8b**, **8c**, **9a**) and 2160 (**5a**, **6a**, **6b**, **7b**, **8a**, **8d**) oscillation images, covering a whole sphere of 6° < 2θ < 55° were corrected by the ω-scan method [–62° < ω < 118° (**5a**, **6a**, **6b**, **7b**, **8a**, **8d**), –70° < ω < 110° (**7a**, **8b**, **8c**, **9a**, **9b**, **10a**, **10b**)] with $\Delta\omega$ of 0.25° (**5a**, **6a**, **6b**, **7b**, **8a**, **8d**) and 0.5° (**7a**, **8b**, **8c**, **9a**, **9b**, **10a**, **10b**). The crystal-to-detector distance was set at 45 (**7a**, **8b**, **8c**, **9a**, **9b**, **10a**, **10b**), 60 (**5a**, **6a**, **6b**, **7b**, **8a**, **8d**) mm. The data were processed using the *Crystal Clear 1.3.5* program (Rigaku/MSC)[14] and corrected for Lorentz-polarization and absorption effects.[15] The structures of complexes were solved by *SHELXL-97*[16] (**4a**, **6a**, **6b**, **7a**) and *SIR-92*[17] (**7b**, **8a**, **8b**, **8c**, **8d**, **9a**, **9b**, **10a**, **10b**) and were refined on F^2 with full-matrix least-squares techniques with *SHELXL-2014/7*[16] using *Crystal Structure 4.2* package.[18] All non-hydrogen atoms were refined with anisotropic thermal parameters and the C-H hydrogen atoms were calculated at ideal positions and refined with riding models. All calculations were carried out on a Pentium PC with *Crystal Structure 4.2* package.[18] In the crystals of **5a**, **6a**, and **6b** solvated molecules were found to be severely disordered and the dispersed electron density in the voids were removed by *SQUEEZE* (*PLATON*)[19] to improve the main part of structures.

CCDC 1485628 (for **5a**), 1485629 (for **6a**), 1485630 (for **6b**), 1485631 (for **7a**), 1485632 (for **7b**), 1485633 (for **8a**), 1485634 (for **8b**), 1485635 (for **8c**), 1485636 (for **8d**), 1485637 (for **9a**), 1485638 (for **9b**), 1485639 (for **10a**), and 1485640 (for **10b**) contain the supplementary crystallographic data for this paper. These data can be obtained free of charge from The Cambridge Crystallographic Data Centre.

Supporting Information (see footnote on the first page of this article): Tables, figures, and CIF files giving the structural parameters for compounds **5**–**10**, ORTEP diagrams of **6b**, **7b**, **8c**,**b**,**d**, **9a**,**b**, and **10a**,**b** as well as ^1H NMR spectra of **5a**,**b**, and **8a**–**d**, and ESI-MS of **5**–**9**.

Acknowledgments

This work was supported by a Grant-in-Aid for Scientific Research and on Priority Area 2107 from the Ministry of Education, Culture, Sports, Science and Technology (MEXT), Japan. T. N. is grateful to Tokuyama Science Foundation, Kurata Memorial Hitachi Science and Technology Foundation, and Nara Women's University for a research project grant.

Keywords: Heterometallic complexes · Dinuclear complexes · Rhodium · Iridium · N,S ligands

[1] a) R. J. Puddephatt, *Chem. Soc. Rev.* **1983**, *12*, 99–127; b) M. E. Broussard, B. Juma, S. G. Train, W.-J. Peng, S. A. Laneman, G. G. Stanley, *Science* **1993**, *260*, 1784–1788; c) A. Bader, E. Linder, *Coord. Chem. Rev.* **1991**, *108*, 27–110; d) C. A. Bessel, P. Aggarwal, A. C. Marschilok, K. J. Takeuchi, *Chem. Rev.* **2001**, *101*, 1031–1066.

[2] For recent examples, see: a) R. B. Siedschlag, V. Bernales, K. D. Vogiatzis, N. Planas, L. J. Clouston, E. Bill, L. Gagliardi, C. C. Lu, *J. Am. Chem. Soc.* **2015**, *137*, 4638–4641; b) Y. Matano, T. Miyajima, T. Nakabuchi, H. Imahori, N. Ochi, S. Sakaki, *J. Am. Chem. Soc.* **2006**, *128*, 11760–11761; c) M. Gagliardo, N. Selander, N. C. Mehendale, G. van Koten, R. J. M. K. Gebbink, K. J. Szabó, *Chem. Eur. J.* **2008**, *14*, 4800–4809; d) C.-C. Lee, W.-C. Ke, K.-T. Chan, C.-L. Lai, C.-H. Hu, H. M. Lee, *Chem. Eur. J.* **2007**, *13*, 582–591; e) V. Miranda-Soto, D. B. Grotjahn, A. G. Dipasquale, A. L. Rheingold, *J. Am. Chem. Soc.* **2008**, *130*, 13200–13201; f) L. J. Hounjet, M. Bierrenstiel, M. J. Ferguson, R. McDonald, M. Cowie, *Dalton Trans.* **2009**, 4213–4226; g) M. R. Kita, A. J. M. Miller, *J. Am. Chem. Soc.* **2014**, *136*, 14519–14529; h) R. Lindner, B. van den Bosch, M. Lutz, J. N. H. Reek, J. I. van der Vlugt, *Organometallics* **2011**, *30*, 499–510.

[3] For our recent examples, see: a) T. Tanase, K. Koike, M. Uegaki, S. Hatada, K. Nakamae, B. Kure, Y. Ura, T. Nakajima, *Dalton Trans.* **2016**, *45*, 7209–7214; b) T. Nakajima, S. Noda, M. Sakamoto, A. Matsui, K. Nakamae, B. Kure, Y. Ura, T. Tanase, *Dalton Trans.* **2016**, *45*, 4747–4761; c) T. Tanase,

M. Chikanishi, K. Morita, K. Nakamae, B. Kure, T. Nakajima, *Chem. Asian J.* **2015**, *10*, 2619–2623; d) T. Tanase, S. Hatada, S. Noda, H. Takenaka, K. Nakamae, B. Kure, T. Nakajima, *Inorg. Chem.* **2015**, *54*, 8298–8309; e) K. Nakamae, Y. Takemura, B. Kure, T. Nakajima, Y. Kitagawa, T. Tanase, *Angew. Chem. Int. Ed.* **2015**, *54*, 1016–1021; *Angew. Chem.* **2015**, *127*, 1030; f) K. Nakamae, B. Kure, T. Nakajima, U. Ura, T. Tanase, *Chem. Asian J.* **2014**, *9*, 3106–3110; g) T. Nakajima, M. Tsuji, N. Hamada, Y. Fukushima, B. Kure, T. Tanase, *J. Organomet. Chem.* **2014**, *768*, 61–67; h) B. Kure, M. Sano, T. Nakajima, T. Tanase, *Organometallics* **2014**, *33*, 3950–3965; i) E. Goto, R. A. Begum, C. Ueno, A. Hosokawa, C. Yamamoto, K. Nakamae, B. Kure, T. Nakajima, T. Tanase, *Organometallics* **2014**, *33*, 1893–1904; j) T. Tanase, R. Otaki, T. Nishida, H. Takenaka, Y. Takemura, B. Kure, T. Nakajima, Y. Kitagawa, T. Tsubomura, *Chem. Eur. J.* **2014**, *20*, 1577–1596; k) T. Tanase, S. Hatada, A. Mochizuki, K. Nakamae, B. Kure, T. Nakajima, *Dalton Trans.* **2013**, *42*, 15941–15952; l) T. Nakajima, M. Sakamoto, S. Kurai, B. Kure, T. Tanase, *Chem. Commun.* **2013**, *49*, 5250–5252; m) B. Kure, T. Nakajima, T. Tanase, *J. Organomet. Chem.* **2013**, *733*, 28–35; n) E. Goto, R. Begum, A. Hosokawa, C. Yamamoto, B. Kure, T. Nakajima, T. Tanase, *Organometallics* **2012**, *31*, 8482–8497; o) B. Kure, A. Taniguchi, T. Nakajima, T. Tanase, *Organometallics* **2012**, *31*, 4791–4800; p) T. Nakajima, S. Kurai, S. Noda, M. Zouda, B. Kure, T. Tanase, *Organometallics* **2012**, *31*, 4283–4294; q) A. Yoshii, H. Takenaka, H. Nagata, S. Noda, K. Nakamae, B. Kure, T. Nakajima, T. Tanase, *Organometallics* **2012**, *31*, 133–143; r) Y. Takemura, H. Takenaka, T. Nakajima, T. Tanase, *Angew. Chem. Int. Ed.* **2009**, *48*, 2157–2161; *Angew. Chem.* **2009**, *121*, 2191; s) T. Tanase, A. Yoshii, R. Otaki, K. Nakamae, Y. Mikita, B. Kure, T. Nakajima, *J. Organomet. Chem.* **2015**, *797*, 37–45.

[4] For recent examples, see: a) R. Angamuthu, P. Byers, M. Lutz, A. L. Spek, E. Bouwman, *Science* **2010**, *327*, 313–315; b) S. Ogo, R. Kabe, K. Uehara, B. Kure, T. Nishimura, S. C. Menon, R. Harada, S. Fukuzumi, Y. Higuchi, T. Ohhara, T. Tamada, R. Kuroki, *Science* **2007**, *316*, 585–587; c) S. Ogo, K. Ichikawa, T. Kishima, T. Matsumoto, H. Nakai, K. Kusaka, T. Ohhara, *Science* **2013**, *339*, 682–684; d) S. Kim, J. Y. Lee, R. E. Cowley, J. W. Ginsbach, M. A. Siegler, E. I. Solomon, K. D. Karlin, *J. Am. Chem. Soc.* **2015**, *137*, 2796–2799; e) P. A. Dub, B. L. Scott, J. C. Gordon, *Organometallics* **2015**, *34*, 4464; f) E. C. M. Ording-Wenker, M. van der Plas, M. A. Siegler, C. F. Guerra, E. Bouwman, *Chem. Eur. J.* **2014**, *20*, 16913–16921; g) C.-W. Chiang, Y.-L. Chu, H.-L. Chen, T.-S. Kuo, W.-Z. Lee, *Chem. Eur. J.* **2014**, *20*, 6283–6286; h) C. Bazzicalupi, C. Caltagirone, Z. Cao, Q. Chen, C. D. Natale, A. Garau, V. Lippolis, L. Lvvova, H. Liu, I. Lundström, M. C. Mostallino, M. Nieddu, R. Paolesse, L. Prodi, M. Sgarzi, N. Zaccheroni, *Chem. Eur. J.* **2013**, *19*, 14639–14653; i) P. Bagchi, T. Morgan, J. Bacsa, C. J. Fahrni, *J. Am. Chem. Soc.* **2013**, *135*, 18549–18559; j) A. M. Thomas, B.-L. Lin, E. C. Wasinger, T. D. P. Stack, *J. Am. Chem. Soc.* **2013**, *135*, 18912–18919; k) P. R. Martínez-Alanis, B. N. S. Eguía, V. M. Ugalde-Saldívar, I. Regla, P. Demare, G. Aullón, I. Castillo, *Chem. Eur. J.* **2013**, *19*, 6067–6079; l) F. Saleem, G. K. Rao, A. Kumar, G. Mukherjee, A. K. Singh, *Organometallics* **2013**, *32*, 3595–3603; m) S. Maji, J. C.-M. Lee, Y.-J. Lu, C.-L. Chen, M.-C. Hung, P. P.-Y. Chen, S. S.-F. Yu, S. I. Chan, *Chem. Eur. J.* **2012**, *18*, 3955–3968; n) M. Ito, A. Watanabe, Y. Shibata, T. Ikariya, *Organometallics* **2010**, *29*, 4584–4592; o) C. A. Bell, P. V. Bernhardt, L. R. Gahan, M. Martínez, M. J. Monteiro, C. Rodríguez, C. A. Sharrad, *Chem. Eur. J.* **2010**, *16*, 3166–3175; p) P. Singh, A. K. Singh, *Organometallics* **2010**, *29*, 6433–6442; q) W. D. Dougherty, K. Rangan, M. J. O'Hagan, G. P. A. Yap, C. G. Riordan, *J. Am. Chem. Soc.* **2008**, *130*, 13510–13511; r) E. Almaraz, Q. A. de Paula, Q. Liu, J. H. Reibenspies, M. Y. Darensbourg, N. P. Farrell, *J. Am. Chem. Soc.* **2008**, *130*, 6272–6280; s) A. Jabri, C. Temple, P. Crewdson, S. Gambarotta, I. Korobkov, R. Duchateau, *J. Am. Chem. Soc.* **2006**, *128*, 9238–9247; t) M. V. Rampersad, S. P. Jeffery, M. L. Golden, J. Lee, J. H. Reibenspies, D. J. Darensbourg, M. Y. Darensbourg, *J. Am. Chem. Soc.* **2005**, *127*, 17323–17334; u) P. V. Rao, S. Bhaduri, J. Jiang, D. Hong, R. H. Holm, *J. Am. Chem. Soc.* **2005**, *127*, 1933–1945.

[5] a) A. E. Roa, J. Campos, M. Paneque, V. Salazar, A. Otero, A. L.-Sánchez, A. M. Rodriguez, I. L.-Solera, M. V. Gómez, *Dalton Trans.* **2015**, *44*, 6987–6998; b) M. Kalidasan, R. Nagarajaprakash, S. Forbes, Y. Mozharivskyj, K. M. Rao, *Z. Anorg. Allg. Chem.* **2015**, *641*, 715–723; c) N. Raja, N. Devika, G. Gupta, V. L. Nayak, A. Kamal, *J. Organomet. Chem.* **2015**, *794*, 104–114; d) K. Ahlford, J. Ekström, A. B. Zaitsev, P. Ryberg, L. Eriksson, H. Adolfsson, *Chem. Eur. J.* **2009**, *15*, 11197–11209; e) H. Wang, X.-Q. Guo, R. Zhong, Y.-J. Lin, P.-C. Zhang, X.-F. Hou, *J. Organomet. Chem.* **2009**, *694*, 3362–3368; f) Y.-F. Han, Y.-J. Lin, W.-G. Jia, G.-X. Jin, *Dalton Trans.* **2009**, 2077–2080; g) S. Liu, H. Wang, P.-C. Zhang, L.-H. Weng, X.-F. Hou, *Organometallics* **2008**, *27*, 713–717; h) V. R. Anna, R. Pallepogu, Z.-Y. Zhou, M. R. Kollipara, *Inorg. Chim. Acta* **2012**, *387*, 37–44; i) M. Trivedi, D. S. Pandey, R.-Q. Zou, Q. Xu, *Inorg. Chem. Commun.* **2008**, *11*, 526–530; j) X. Wang, G.-X. Jin, *Chem. Eur. J.* **2005**, *11*, 5758–5764; k) P. Piraino, G. Giuseppe, G. Faraone, G. Bombieri, *J. Chem. Soc., Dalton Trans.* **1983**, 2391–2395.

[6] a) O. Prakash, H. Joshi, N. N. Sharma, P. L. Gupta, A. K. Singh, *Organometallics* **2014**, *33*, 3804–3812; b) F. Saleem, G. K. Rao, A. Kumar, G. Mukherjee, A. K. Singh, *Organometallics* **2014**, *33*, 2341–2351; c) S. Hohloch, L. Hettmanczyk, B. Sarkar, *Eur. J. Inorg. Chem.* **2014**, 3164–3171; d) O. Prakash, P. Singh, G. Mukherjee, A. K. Singh, *Organometallics* **2012**, *31*, 3379–3388; e) S. Ye, W. Kaim, M. Albrecht, F. Lissner, T. Schleid, *Inorg. Chim. Acta* **2004**, *357*, 3325–3330; f) M. Albrecht, T. Scheiring, T. Sixt, W. Kaim, *J. Organomet. Chem.* **2000**, *596*, 84–89.

[7] a) H. Brunner, A. Köllnberger, A. Mehmood, T. Tsuno, M. Zabel, *J. Organomet. Chem.* **2004**, *689*, 4244–4262; b) H. Brunner, H. Ike, M. Muschiol, T. Tsuno, K. Koyama, T. Kurosawa, M. Zabel, *Organometallics* **2011**, *30*, 3666–3676; c) H. Brunner, M. Muschiol, T. Tsuno, H. Ike, T. Kurosawa, K. Koyama, *Angew. Chem. Int. Ed.* **2012**, *51*, 1067–1070; *Angew. Chem.* **2012**, *124*, 1092; d) H. Brunner, T. Tsuno, *Acc. Chem. Res.* **2009**, *42*, 1501–1510.

[8] T. Nakajima, Y. Fukushima, M. Tsuji, N. Hamada, B. Kure, T. Tanase, *Organometallics* **2013**, *32*, 7470–7477.

[9] S. J. Mountford, R. Daly, A. J. Robinson, M. T. W. Hearn, *J. Chromatogr. A* **2014**, *1355*, 15–25.

[10] a) L. Baradello, S. L. Schiavo, F. Nicoló, S. Lanza, G. Alibrandi, G. Tresoldi, *Eur. J. Inorg. Chem.* **2004**, 3358–3369; b) G. Tresoldi, S. L. Schiavo, S. Lanza, P. Cardiano, *Eur. J. Inorg. Chem.* **2002**, 181–191; c) E. W. Abel, P. J. Heard, K. G. Orrell, M. B. Hursthouse, M. A. Mazid, *J. Chem. Soc., Dalton Trans.* **1993**, 3795–3801; d) E. A. Abel, D. Ellis, K. G. Orrell, *J. Chem. Soc., Dalton Trans.* **1992**, 2243–2249.

[11] D. Carmona, M. P. Lamata, F. Viguri, R. Rodríguez, F. J. Lahoz, I. T. Dobrinovitch, L. A. Oro, *Dalton Trans.* **2007**, 1911–1921.

[12] C. K. Jørgensen, *Prog. Inorg. Chem.* **1962**, *4*, 73–124.

[13] a) A. Takayama, T. Suzuki, M. Ikeda, Y. Sunatsuki, M. Kojima, *Dalton Trans.* **2013**, *42*, 14556–14567; b) T. Nakagawa, H. Seino, Y. Mizobe, *J. Organomet. Chem.* **2010**, *695*, 137–144; c) Y. Takahashi, N. Murakami, K. Fujita, R. Yamaguchi, *Dalton Trans.* **2009**, 2029–2042; d) Y. Yamamoto, S. Sakamoto, Y. Ohki, A. Usuzawa, M. Fujita, T. Mochida, *Dalton Trans.* **2003**, 3534–3540; e) Y. Yamamoto, F. Miyauchi, *Inorg. Chim. Acta* **2002**, *334*, 77–90.

[14] *Crystal Clear*, version 1.3.5, *Operating software for the CCD detector system*, Rigaku and Molecular Structure Corp., Tokyo, Japan, and The Woodlands, Texas, USA, **2003**.

[15] R. Jacobson, *REQAB*, Molecular Structure Corporation, The Woodlands, Texas, USA, **1998**.

[16] G. M. Sheldrick, *SHELXL-97: Program for the Refinement of Crystal Structures*, University of Göttingen, Germany, **1996**.

[17] A. Altomare, M. C. Burla, M. Camalli, M. Cascarano, C. Giacovazzo, A. Guagliardi, G. Polidori, *J. Appl. Crystallogr.* **1994**, *27*, 435–436.

[18] *CrystalStructure*, version 4.1, *Crystal Structure Analysis Package*, Rigaku Corporation, Tokyo 196-8666, Japan, **2000**–**2010**.

[19] A. L. Spek, *Acta Crystallogr., Sect. D* **2009**, *65*, 148.

Received: July 19, 2016
Published Online: ■

Mixed Donor Ligands

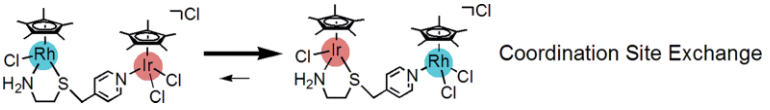

Coordination-site exchange reactions of Cp*M (M = Rh, Ir) fragments occurred in homo- and heterodinuclear Rh^{III} and Ir^{III} complexes supported by a SN_2 Ligand.

DOI: 10.1002/ejic.201600722